3

Pulse Propagation in Dispersive Media

In this chapter, we examine some aspects of pulse propagation in dispersive media and the role played by various wave velocity definitions, such as phase, group, and front velocities. We discuss group velocity dispersion, pulse spreading, chirping, and dispersion compensation, and look at some slow, fast, and negative group velocity examples. We also present a short introduction to chirp radar and pulse compression, elaborating on the similarities to dispersion compensation. The similarities to Fresnel diffraction and Fourier optics are discussed in Sec. 17.18. The chapter ends with a guide to the literature in these diverse topics.

3.1 Propagation Filter

As we saw in the previous chapter, a monochromatic plane wave moving forward along the z-direction has an electric field $E(z) = E(0)e^{-jkz}$, where $E(z)$ stands for either the x or the y component. We assume a homogeneous isotropic non-magnetic medium ($\mu = \mu_0$) with an effective permittivity $\epsilon(\omega)$; therefore, k is the frequency-dependent and possibly complex-valued wavenumber defined by $k(\omega) = \omega\sqrt{\epsilon(\omega)\mu_0}$. To emphasize the dependence on the frequency ω, we rewrite the propagated field as:[†]

$$\hat{E}(z, \omega) = e^{-jkz}\hat{E}(0, \omega) \tag{3.1.1}$$

Its complete space-time dependence will be:

$$e^{j\omega t}\hat{E}(z, \omega) = e^{j(\omega t - kz)}\hat{E}(0, \omega) \tag{3.1.2}$$

A wave packet or pulse can be made up by adding different frequency components, that is, by the inverse Fourier transform:

$$E(z, t) = \frac{1}{2\pi}\int_{-\infty}^{\infty} e^{j(\omega t - kz)}\hat{E}(0, \omega)\, d\omega \tag{3.1.3}$$

[†]where the hat denotes Fourier transformation.

Setting $z = 0$, we recognize $\hat{E}(0, \omega)$ to be the Fourier transform of the initial waveform $E(0, t)$, that is,

$$E(0, t) = \frac{1}{2\pi}\int_{-\infty}^{\infty} e^{j\omega t}\hat{E}(0, \omega)\, d\omega \quad \Leftrightarrow \quad \hat{E}(0, \omega) = \int_{-\infty}^{\infty} e^{-j\omega t}E(0, t)\, dt \tag{3.1.4}$$

The multiplicative form of Eq. (3.1.1) allows us to think of the propagated field as the output of a *linear system*, the propagation filter, whose frequency response is

$$\boxed{H(z, \omega) = e^{-jk(\omega)z}} \tag{3.1.5}$$

Indeed, for a linear time-invariant system with impulse response $h(t)$ and corresponding frequency response $H(\omega)$, the input/output relationship can be expressed multiplicatively in the frequency domain or convolutionally in the time domain:

$$\hat{E}_{\text{out}}(\omega) = H(\omega)\hat{E}_{\text{in}}(\omega)$$

$$E_{\text{out}}(t) = \int_{-\infty}^{\infty} h(t - t')E_{\text{in}}(t')\, dt'$$

For the propagator frequency response $H(z, \omega) = e^{-jk(\omega)z}$, we obtain the corresponding impulse response:

$$\boxed{h(z, t) = \frac{1}{2\pi}\int_{-\infty}^{\infty} e^{j\omega t}H(z, \omega)\, d\omega = \frac{1}{2\pi}\int_{-\infty}^{\infty} e^{j(\omega t - kz)}\, d\omega} \tag{3.1.6}$$

Alternatively, Eq. (3.1.6) follows from (3.1.3) by setting $\hat{E}(0, \omega) = 1$, corresponding to an impulsive input $E(0, t) = \delta(t)$. Thus, Eq. (3.1.3) may be expressed in the time domain in the convolutional form:

$$\boxed{E(z, t) = \int_{-\infty}^{\infty} h(z, t - t')E(0, t')\, dt'} \tag{3.1.7}$$

Example 3.1.1: For propagation in a dispersionless medium with frequency-independent permittivity, such as the vacuum, we have $k = \omega/c$, where $c = 1/\sqrt{\mu\epsilon}$. Therefore,

$$H(z, \omega) = e^{-jk(\omega)z} = e^{-j\omega z/c} = \text{pure delay by } z/c$$

$$h(z, t) = \frac{1}{2\pi}\int_{-\infty}^{\infty} e^{j(\omega t - kz)}\, d\omega = \frac{1}{2\pi}\int_{-\infty}^{\infty} e^{j\omega(t - z/c)}\, d\omega = \delta(t - z/c)$$

and Eq. (3.1.7) gives $E(z, t) = E(0, t - z/c)$, in agreement with the results of Sec. 2.1.   □

The reality of $h(z, t)$ implies the hermitian property, $H(z, -\omega)^* = H(z, \omega)$, for the frequency response, which is equivalent to the anti-hermitian property for the wavenumber, $k(-\omega)^* = -k(\omega)$.

3.2 Front Velocity and Causality

For a general linear system $H(\omega) = |H(\omega)|e^{-j\phi(\omega)}$, one has the standard concepts of phase delay, group delay, and signal-front delay [178] defined in terms of the system's phase-delay response, that is, the negative of its phase response, $\phi(\omega) = -\text{Arg}\,H(\omega)$:

$$t_p = \frac{\phi(\omega)}{\omega}\,,\quad t_g = \frac{d\phi(\omega)}{d\omega}\,,\quad t_f = \lim_{\omega\to\infty}\frac{\phi(\omega)}{\omega} \tag{3.2.1}$$

The significance of the signal-front delay t_f for the causality of a linear system is that the impulse response vanishes, $h(t) = 0$, for $t < t_f$, which implies that if the input begins at time $t = t_0$, then the output will begin at $t = t_0 + t_f$:

$$E_{\text{in}}(t) = 0 \text{ for } t < t_0 \quad\Rightarrow\quad E_{\text{out}}(t) = 0 \text{ for } t < t_0 + t_f \tag{3.2.2}$$

To apply these concepts to the propagator filter, we write $k(\omega)$ in terms of its real and imaginary parts, $k(\omega) = \beta(\omega) - j\alpha(\omega)$, so that

$$H(z,\omega) = e^{-jk(\omega)z} = e^{-\alpha(\omega)z}e^{-j\beta(\omega)z} \quad\Rightarrow\quad \phi(\omega) = \beta(\omega)z \tag{3.2.3}$$

Then, the definitions (3.2.1) lead naturally to the concepts of phase velocity, group velocity, and signal-front velocity, defined through:

$$t_p = \frac{z}{v_p}\,,\quad t_g = \frac{z}{v_g}\,,\quad t_f = \frac{z}{v_f} \tag{3.2.4}$$

For example, $t_g = d\phi/d\omega = (d\beta/d\omega)z = z/v_g$, and similarly for the other ones, resulting in the definitions:

$$v_p = \frac{\omega}{\beta(\omega)}\,,\quad v_g = \frac{d\omega}{d\beta}\,,\quad v_f = \lim_{\omega\to\infty}\frac{\omega}{\beta(\omega)} \tag{3.2.5}$$

The expressions for the phase and group velocities agree with those of Sec. 1.18. Under the reasonable assumption that $\epsilon(\omega) \to \epsilon_0$ as $\omega \to \infty$, which is justified on the basis of the permittivity model of Eq. (1.11.11), we have $k(\omega) = \omega\sqrt{\epsilon(\omega)\mu_0} \to \omega\sqrt{\epsilon_0\mu_0} = \omega/c$, where c is the speed of light in vacuum. Therefore, the signal front velocity and front delay are:

$$v_f = \lim_{\omega\to\infty}\frac{\omega}{\beta(\omega)} = \lim_{\omega\to\infty}\frac{\omega}{\omega/c} = c \quad\Rightarrow\quad t_f = \frac{z}{c} \tag{3.2.6}$$

Thus, we expect that the impulse response $h(z,t)$ of the propagation medium would satisfy the causality condition:

$$h(z,t) = 0\,,\quad\text{for}\quad t < t_f = \frac{z}{c} \tag{3.2.7}$$

We show this below. More generally, if the input pulse at $z = 0$ vanishes for $t < t_0$, the propagated pulse to distance z will vanish for $t < t_0 + z/c$. This is the statement of *relativistic causality*, that is, if the input signal has a sharp, discontinuous, front at
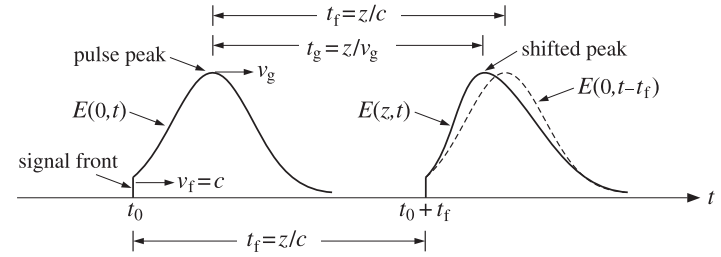

Fig. 3.2.1 Causal pulse propagation, but with superluminal group velocity ($v_g > c$).

some time t_0, then that front cannot move faster than the speed of light in vacuum and cannot reach the point z faster than z/c seconds later. Mathematically,

$$E(0,t) = 0 \text{ for } t < t_0 \quad\Rightarrow\quad E(z,t) = 0 \text{ for } t < t_0 + \frac{z}{c} \tag{3.2.8}$$

Fig. 3.2.1 depicts this property. Sommerfeld and Brillouin [177,1135] originally showed this property for a causal sinusoidal input, that is, $E(0,t) = e^{j\omega_0 t}u(t)$.

Group velocity describes the speed of the peak of the envelope of a signal and is a concept that applies only to narrow-band pulses. As mentioned in Sec. 1.18, it is possible that if this narrow frequency band is concentrated in the vicinity of an anomalous dispersion region, that is, near an absorption peak, the corresponding group velocity will exceed the speed of light in vacuum, $v_g > c$, or even become negative depending on the value of the negative slope of the refractive index $dn_r/d\omega < 0$.

Conventional wisdom has it that the condition $v_g > c$ is not at odds with relativity theory because the strong absorption near the resonance peak causes severe distortion and attenuation of the signal peak and the group velocity loses its meaning. However, in recent years it has been shown theoretically and experimentally [251,252,270] that the group velocity can retain its meaning as representing the speed of the peak even if v_g is superluminal or negative. Yet, relativistic causality is preserved because the signal front travels with the speed of light. It is the sharp discontinuous front of a signal that may convey information, not necessarily its peak. Because the pulse undergoes continuous reshaping as it propagates, the front cannot be overtaken by the faster moving peak.

This is explained pictorially in Fig. 3.2.1 which depicts such a case where $v_g > c$, and therefore, $t_g < t_f$. For comparison, the actual field $E(z,t)$ is shown together with the input pulse as if the latter had been traveling in vacuum, $E(0, t - z/c)$, reaching the point z with a delay of $t_f = z/c$. The peak of the pulse, traveling with speed v_g, gets delayed by the group delay t_g when it arrives at distance z. Because $t_g < t_f$, the peak of $E(z,t)$ shifts forward in time and occurs *earlier* than it would if the pulse were traveling in vacuum. Such peak shifting is a consequence of the "filtering" or "rephasing" taking place due to the propagator filter's frequency response $e^{-jk(\omega)z}$.

The causality conditions (3.2.7) and (3.2.8) imply that the value of the propagated field $E(z,t)$ at some time instant $t > t_0 + z/c$ is determined only by those values of the input pulse $E(0,t')$ that are z/c seconds earlier, that is, for $t_0 \le t' \le t - z/c$. This follows from the convolutional equation (3.1.7): the factor $h(z, t - t')$ requires that

$t - t' \geq z/c$, the factor $E(0, t')$ requires $t' \geq t_0$, yielding $t_0 \leq t' \leq t - z/c$. Thus,

$$E(z, t) = \int_{t_0}^{t - z/c} h(z, t - t') E(0, t') dt', \quad \text{for} \quad t > t_0 + z/c \qquad (3.2.9)$$

For example, the value of $E(z, t)$ at $t = t_1 + t_f = t_1 + z/c$ is given by:

$$E(z, t_1 + t_f) = \int_{t_0}^{t_1} h(z, t_1 + t_f - t') E(0, t') dt'$$

Thus, as shown in Fig. 3.2.2, the shaded portion of the input $E(0, t')$ over the time interval $t_0 \leq t' \leq t_1$ determines causally the shaded portion of the propagated signal $E(z, t)$ over the interval $t_0 + t_f \leq t \leq t_1 + t_f$. The peaks, on the other hand, are not causally related. Indeed, the interval $[t_0, t_1]$ of the input does not include the peak, whereas the interval $[t_0 + t_f, t_1 + t_f]$ of the output does include the (shifted) peak.
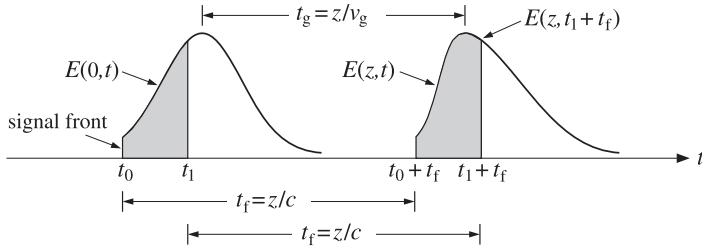

Fig. 3.2.2 Shaded areas show causally related portions of input and propagated signals.

Next, we provide a justification of Eq. (3.2.8). The condition $E(0, t) = 0$ for $t < t_0$, implies that its Fourier transform is:

$$\hat{E}(0, \omega) = \int_{t_0}^{\infty} e^{-j\omega t} E(0, t) dt \quad \Rightarrow \quad e^{j\omega t_0} \hat{E}(0, \omega) = \int_0^{\infty} e^{-j\omega t} E(0, t + t_0) dt \quad (3.2.10)$$

where the latter equation was obtained by the change of integration variable from t to $t + t_0$. It follows now that $e^{j\omega t_0} \hat{E}(0, \omega)$ is analytically continuable into the lower-half ω-plane. Indeed, the replacement $e^{-j\omega t}$ by $e^{-j(\omega - j\sigma)t} = e^{-\sigma t} e^{-j\omega t}$ with $\sigma > 0$ and $t > 0$, improves the convergence of the time integral in (3.2.10). We may write now Eq. (3.1.3) in the following form:

$$E(z, t) = \frac{1}{2\pi} \int_{-\infty}^{\infty} e^{j(\omega t - \omega t_0 - kz)} e^{j\omega t_0} \hat{E}(0, \omega) d\omega \qquad (3.2.11)$$

and assume that $t < t_0 + z/c$. A consequence of the permittivity model (1.11.11) is that the wavenumber $k(\omega)$ has singularities only in the upper-half ω-plane and is analytic in the lower half. For example, for the single-resonance case, we have:

$$\epsilon(\omega) = \epsilon_0 \left[1 + \frac{\omega_p^2}{\omega_0^2 - \omega^2 + j\omega\gamma} \right] \quad \Rightarrow \quad \begin{aligned} \text{zeros} &= \frac{j\gamma}{2} \pm \sqrt{\omega_0^2 + \omega_p^2 - \frac{\gamma^2}{4}} \\ \text{poles} &= \frac{j\gamma}{2} \pm \sqrt{\omega_0^2 - \frac{\gamma^2}{4}} \end{aligned}$$

Thus, the integrand of Eq. (3.2.11) is analytic in the lower-half ω-plane and we may replace the integration path along the real axis by the lower semi-circular counterclockwise path C_R at a very large radius R, as shown below:

$$E(z, t) = \frac{1}{2\pi} \int_{-\infty}^{\infty} e^{j(\omega t - \omega t_0 - kz)} e^{j\omega t_0} \hat{E}(0, \omega) d\omega$$

$$= \lim_{R \to \infty} \frac{1}{2\pi} \int_{C_R} e^{j(\omega t - \omega t_0 - kz)} e^{j\omega t_0} \hat{E}(0, \omega) d\omega$$
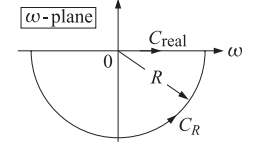
But for large ω, we may replace $k(\omega) = \omega/c$. Thus,

$$E(z, t) = \lim_{R \to \infty} \frac{1}{2\pi} \int_{C_R} e^{j\omega(t - t_0 - z/c)} e^{j\omega t_0} \hat{E}(0, \omega) d\omega$$

Because $t - t_0 - z/c < 0$, and under the mild assumption that $e^{j\omega t_0} \hat{E}(0, \omega) \to 0$ for $|\omega| = R \to \infty$ in the lower-half plane, it follows from the Jordan lemma that the above integral will be zero. Therefore, $E(z, t) = 0$ for $t < t_0 + z/c$.

As an example, consider the signal $E(0, t) = e^{-a(t - t_0)} e^{j\omega_0(t - t_0)} u(t - t_0)$, that is, a delayed exponentially decaying ($a > 0$) causal sinusoid. Its Fourier transform is

$$\hat{E}(0, \omega) = \frac{e^{-j\omega t_0}}{j(\omega - \omega_0 - ja)} \quad \Rightarrow \quad e^{j\omega t_0} \hat{E}(0, \omega) = \frac{1}{j(\omega - \omega_0 - ja)}$$

which is analytic in the lower half-plane and converges to zero for $|\omega| \to \infty$.

The proof of Eq. (3.2.7) is similar. Because of the analyticity of $k(\omega)$, the integration path in Eq. (3.1.6) can again be replaced by C_R, and $k(\omega)$ replaced by ω/c:

$$h(z, t) = \lim_{R \to \infty} \frac{1}{2\pi} \int_{C_R} e^{j\omega(t - z/c)} d\omega, \quad \text{for} \quad t < z/c$$

This integral can be done exactly,[†] and leads to a standard representation of the delta function:

$$h(z, t) = \lim_{R \to \infty} \frac{\sin(R(t - z/c))}{\pi(t - z/c)} = \delta(t - z/c)$$

which vanishes since we assumed that $t < z/c$. For $t > z/c$, the contour in (3.1.6) can be closed in the upper half-plane, but its evaluation requires knowledge of the particular singularities of $k(\omega)$.

3.3 Exact Impulse Response Examples

Some exactly solvable examples are given in [184]. They are all based on the following Fourier transform pair, which can be found in [179]:[‡]

$$H(z, \omega) = e^{-jk(\omega)z} = e^{-t_f \sqrt{j\omega + a + b} \sqrt{j\omega + a - b}}$$

$$h(z, t) = \delta(t - t_f) e^{-at_f} + \frac{I_1\left(b\sqrt{t^2 - t_f^2}\right)}{\sqrt{t^2 - t_f^2}} bt_f e^{-at} u(t - t_f) \qquad (3.3.1)$$

[†] set $\omega = Re^{j\theta}$, $d\omega = jRe^{j\theta} d\theta$, and integrate over $-\pi \leq \theta \leq 0$

[‡] see the pair 863.1 on p. 110 of [179].

where $I_1(x)$ is the modified Bessel function of the first kind of order one, and $t_f = z/c$ is the front delay. The unit step $u(t - t_f)$ enforces the causality condition (3.2.7). From the expression of $H(z, \omega)$, we identify the corresponding wavenumber:

$$k(\omega) = \frac{-j}{c}\sqrt{j\omega + a + b}\,\sqrt{j\omega + a - b} \tag{3.3.2}$$

The following physical examples are described by appropriate choices of the parameters a, b, c in Eq. (3.3.2):

1. $a = 0,\quad b = 0$ — propagation in vacuum or dielectric
2. $a > 0,\quad b = 0$ — weakly conducting dielectric
3. $a = b > 0$ — medium with finite conductivity
4. $a = 0,\quad b = j\omega_p$ — lossless plasma
5. $a = 0,\quad b = j\omega_c$ — hollow metallic waveguide
6. $a + b = R'/L',\quad a - b = G'/C'$ — lossy transmission line

The anti-hermitian property $k(-\omega)^* = -k(\omega)$ is satisfied in two cases: when the parameters a, b are both real, or, when a is real and b imaginary.

In case 1, we have $k = \omega/c$ and $h(z, t) = \delta(t - t_f) = \delta(t - z/c)$. Setting $a = c\alpha > 0$ and $b = 0$, we find for case 2:

$$k = \frac{\omega - ja}{c} = \frac{\omega}{c} - j\alpha \tag{3.3.3}$$

which corresponds to a medium with a constant attenuation coefficient $\alpha = a/c$ and a propagation constant $\beta = \omega/c$, as was the case of a weakly conducting dielectric of Sec. 2.7. In this case c is the speed of light in the dielectric, i.e. $c = 1/\sqrt{\mu\epsilon}$ and a is related to the conductivity σ by $a = c\alpha = \sigma/2\epsilon$. The medium impulse response is:

$$h(z, t) = \delta(t - t_f)e^{-at_f} = \delta(t - z/c)e^{-\alpha z}$$

Eq. (3.1.7) then implies that an input signal will travel at speed c while attenuating with distance:
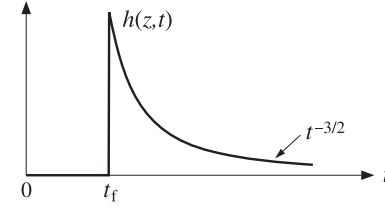
$$E(z, t) = e^{-\alpha z}E(0, t - z/c)$$

Case 3 describes a medium with frequency-independent permittivity and conductivity ϵ, σ with the parameters $a = b = \sigma/2\epsilon$ and $c = 1/\sqrt{\mu_0\epsilon}$. Eq. (3.3.2) becomes:

$$k = \frac{\omega}{c}\sqrt{1 - j\frac{\sigma}{\omega\epsilon}} \tag{3.3.4}$$

and the impulse response is:

$$h(z, t) = \delta(t - z/c)e^{-az/c} + \frac{I_1\left(a\sqrt{t^2 - (z/c)^2}\right)}{\sqrt{t^2 - (z/c)^2}}\,\frac{az}{c}\,e^{-at}\,u(t - z/c) \tag{3.3.5}$$

A plot of $h(z, t)$ for $t > t_f$ is shown below.

For large t, $h(z, t)$ is not exponentially decaying, but falls like $1/t^{3/2}$. Using the large-x asymptotic form $I_1(x) \to e^x/\sqrt{2\pi x}$, and setting $\sqrt{t^2 - t_f^2} \to t$ for $t \gg t_f$, we find

$$h(z, t) \to \frac{e^{at}}{t\sqrt{2\pi at}}\,at_f\,e^{-at} = \frac{at_f}{t\sqrt{2\pi at}},\quad t \gg t_f$$

Case 4 has parameters $a = 0$ and $b = j\omega_p$ and describes propagation in a plasma, where ω_p is the plasma frequency. Eq. (3.3.2) reduces to Eq. (1.15.2):

$$k = \frac{1}{c}\sqrt{\omega^2 - \omega_p^2}$$

To include evanescent waves (having $\omega < \omega_p$), Eq. (3.3.2) may be written in the more precise form that satisfies the required anti-hermitian property $k(-\omega)^* = -k(\omega)$:

$$k(\omega) = \frac{1}{c}\begin{cases} \mathrm{sign}(\omega)\sqrt{\omega^2 - \omega_p^2}, & \text{if } |\omega| \geq \omega_p \\ -j\sqrt{\omega_p^2 - \omega^2}, & \text{if } |\omega| \leq \omega_p \end{cases} \tag{3.3.6}$$

When $|\omega| \leq \omega_p$, the wave is evanescent in the sense that it attenuates exponentially with distance:

$$e^{-jkz} = e^{-z\sqrt{\omega_p^2 - \omega^2}/c}$$

For numerical evaluation using MATLAB, it proves convenient to leave $k(\omega)$ in the form of Eq. (3.3.2), that is,
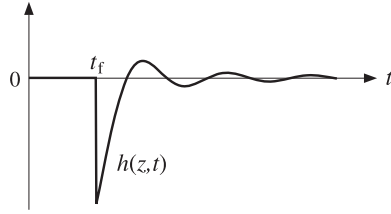
$$k(\omega) = \frac{-j}{c}\sqrt{j(\omega + \omega_p)}\,\sqrt{j(\omega - \omega_p)}$$

which evaluates correctly according to Eq. (3.3.6) using MATLAB's rules for computing square roots (e.g., $\sqrt{\pm j} = e^{\pm j\pi/4}$).

Because b is imaginary, we can use the property $I_1(jx) = jJ_1(x)$, where $J_1(x)$ is the ordinary Bessel function. Thus, setting $a = 0$ and $b = j\omega_p$ in Eq. (3.3.1), we find:

$$h(z, t) = \delta(t - t_f) - \frac{J_1\left(\omega_p\sqrt{t^2 - t_f^2}\right)}{\sqrt{t^2 - t_f^2}}\,\omega_p t_f\,u(t - t_f) \tag{3.3.7}$$

A plot of $h(z, t)$ for $t > t_f$ is shown below.

The propagated output $E(z,t)$ due to a causal input, $E(0,t) = E(0,t)u(t)$, is obtained by convolution, where we must impose the conditions $t' \geq t_f$ and $t - t' \geq 0$:

$$E(z,t) = \int_{-\infty}^{\infty} h(z,t')E(0,t-t')dt'$$

which for $t \geq t_f$ leads to:

$$E(z,t) = E(0,t-t_f) - \int_{t_f}^{t} \frac{J_1\left(\omega_p\sqrt{t'^2 - t_f^2}\right)}{\sqrt{t'^2 - t_f^2}} \, \omega_p t_f \, E(0,t-t')dt' \tag{3.3.8}$$

We shall use Eq. (3.3.8) in the next section to illustrate the transient and steady-state response of a propagation medium such as a plasma or a waveguide. The large-t behavior of $h(z,t)$ is obtained from the asymptotic form:

$$J_1(x) \to \sqrt{\frac{2}{\pi x}} \cos\left(x - \frac{3\pi}{4}\right), \quad x \gg 1$$

which leads to

$$h(z,t) \to -\frac{\sqrt{2\omega_p}\,t_f}{\sqrt{\pi}\,t^{3/2}} \cos\left(\omega_p t - \frac{3\pi}{4}\right), \quad t \gg t_f \tag{3.3.9}$$

Case 5 is the same as case 4, but describes propagation in an air-filled hollow metallic waveguide with cutoff frequency ω_c. We will see in Chap. 9 that the dispersion relationship (3.3.6) is a consequence of the boundary conditions on the waveguide walls, and therefore, it is referred to as *waveguide dispersion*, as opposed to *material dispersion* arising from a frequency-dependent permittivity $\epsilon(\omega)$.

Case 6 describes a lossy transmission line (see Sec. 10.6) with distributed (that is, per unit length) inductance L', capacitance C', series resistance R', and shunt conductance G'. This case reduces to case 3 if $G' = 0$. The corresponding propagation speed is $c = 1/\sqrt{L'C'}$. The ω–k dispersion relationship can be written in the form of Eq. (10.6.5):

$$k = -j\sqrt{(R' + j\omega L')(G' + j\omega C')} = \omega\sqrt{L'C'}\sqrt{\left(1 - j\frac{R'}{\omega L'}\right)\left(1 - j\frac{G'}{\omega C'}\right)}$$

3.4 Transient and Steady-State Behavior

The frequency response $e^{-jk(\omega)z}$ is the Fourier transform of $h(z,t)$, but because of the causality condition $h(z,t) = 0$ for $t < z/c$, the time-integration in this Fourier transform can be restricted to the interval $z/c < t < \infty$, that is,

$$\boxed{e^{-jk(\omega)z} = \int_{z/c}^{\infty} e^{-j\omega t}h(z,t)dt} \tag{3.4.1}$$

We mention, parenthetically, that Eq. (3.4.1), which incorporates the causality condition of $h(z,t)$, can be used to derive the lower half-plane analyticity of $k(\omega)$ and of the corresponding complex refractive index $n(\omega)$ defined through $k(\omega) = \omega n(\omega)/c$. The analyticity properties of $n(\omega)$ can then be used to derive the Kramers-Kronig dispersion relations satisfied by $n(\omega)$ itself [182], as opposed to those satisfied by the susceptibility $\chi(\omega)$ that were discussed in Sec. 1.17.

When a causal sinusoidal input is applied to the linear system $h(z,t)$, we expect the system to exhibit an initial transient behavior followed by the usual sinusoidal steady-state response. Indeed, applying the initial pulse $E(0,t) = e^{j\omega_0 t}u(t)$, we obtain from the system's convolutional equation:

$$E(z,t) = \int_{z/c}^{t} h(z,t')E(0,t-t')dt' = \int_{z/c}^{t} h(z,t')e^{j\omega_0(t-t')}dt'$$

where the restricted limits of integration follow from the conditions $t' \geq z/c$ and $t - t' \geq 0$ as required by the arguments of the functions $h(z,t')$ and $E(0,t-t')$. Thus, for $t \geq z/c$, the propagated field takes the form:

$$E(z,t) = e^{j\omega_0 t}\int_{z/c}^{t} e^{-j\omega_0 t'}h(z,t')dt' \tag{3.4.2}$$

In the steady-state limit, $t \to \infty$, the above integral tends to the frequency response (3.4.1) evaluated at $\omega = \omega_0$, resulting in the standard sinusoidal response:

$$e^{j\omega_0 t}\int_{z/c}^{t} e^{-j\omega_0 t'}h(z,t')dt' \to e^{j\omega_0 t}\int_{z/c}^{\infty} e^{-j\omega_0 t'}h(z,t')dt' = H(z,\omega_0)e^{j\omega_0 t}, \quad \text{or,}$$

$$E_{\text{steady}}(z,t) = e^{j\omega_0 t - jk(\omega_0)z}, \quad \text{for} \quad t \gg z/c \tag{3.4.3}$$

Thus, the field $E(z,t)$ eventually evolves into an ordinary plane wave at frequency ω_0 and wavenumber $k(\omega_0) = \beta(\omega_0) - j\alpha(\omega_0)$. The initial transients are given by the exact equation (3.4.2) and depend on the particular form of $k(\omega)$. They are generally referred to as "precursors" or "forerunners" and were originally studied by Sommerfeld and Brillouin [177,1135] for the case of a single-resonance Lorentz permittivity model.

It is beyond the scope of this book to study the precursors of the Lorentz model. However, we may use the exactly solvable model for a plasma or waveguide given in Eq. (3.3.7) and numerically integrate (3.4.2) to illustrate the transient and steady-state behavior.

Fig. 3.4.1 shows on the left graph the input sinusoid (dotted line) and the steady-state sinusoid (3.4.3) with k_0 computed from (3.3.6). The input and the steady output differ by the phase shift $-k_0 z$. The graph on the right shows the causal output for $t \geq t_f$ computed using Eq. (3.3.8) with the input $E(0,t) = \sin(\omega_0 t)u(t)$. During the initial transient period the output signal builds up to its steady-state form. The steady form of the left graph was not superimposed on the exact output because the two are virtually indistinguishable for large t. The graph units were arbitrary and we chose the following numerical values of the parameters:

$$c = 1 \quad \omega_p = 1, \quad \omega_0 = 3, \quad t_f = z = 10$$

The following MATLAB code illustrates the computation of the exact and steady-state output signals:
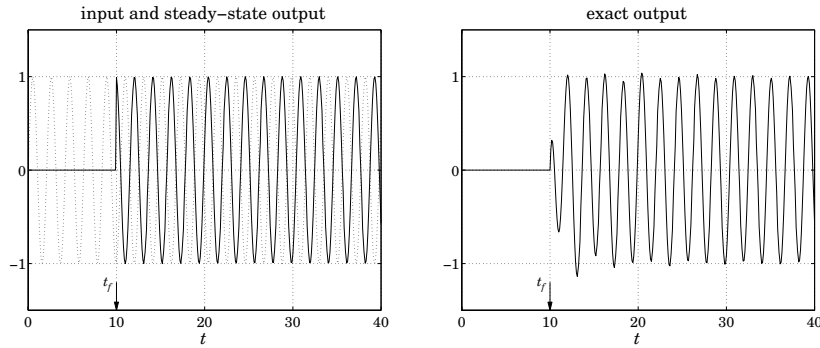
input and steady–state output

exact output

Fig. 3.4.1   Transient and steady-state sinusoidal response.

```
wp = 1; w0 = 3; tf = 10;
k0 = -j * sqrt(j*(w0+wp)) * sqrt(j*(w0-wp));        % equivalent to Eq. (3.3.6)

t = linspace(0,40, 401);

N = 15; K = 20;        % use N-point Gaussian quadrature, dividing [tf,t] into K subintervals

for i=1:length(t),
    if t(i)<tf,
        Ez(i) = 0;
        Es(i) = 0;
    else
        [w,x] = quadrs(linspace(tf,t(i),K), N);        % quadrature weights and points
        h = - wp^2 * tf * J1over(wp*sqrt(x.^2 - tf^2)) .* exp(j*w0*(t(i)-x));
        Ez(i) = exp(j*w0*(t(i)-tf)) + w'*h;        % exact output
        Es(i) = exp(j*w0*t(i)-j*k0*tf);        % steady-state
    end
end

es = imag(Es); ez = imag(Ez);        % input is E(0,t) = sin(w0 t) u(t)

figure; plot(t,es); figure; plot(t,ez);
```

The code uses the function quadrs (see Sec. 18.10 and Appendix I) to compute the integral over the interval $[t_f, t]$, dividing this interval into K subintervals and using an N-point Gauss-Legendre quadrature method on each subinterval.

We wrote a function J1over to implement the function $J_1(x)/x$. The function uses the power series expansion, $J_1(x)/x = 0.5(1 - x^2/8 + x^4/192)$, for small x, and the built-in MATLAB function besselj for larger x:

```
function y = J1over(x)

y = zeros(size(x));        % y has the same size as x

xmin = 1e-4;

i = find(abs(x) < xmin);
```

```
y(i) = 0.5 * (1 - x(i).^2 / 8 + x(i).^4 / 192);

i = find(abs(x) >= xmin);
y(i) = besselj(1, x(i)) ./ x(i);
```

input and steady–state evanescent output
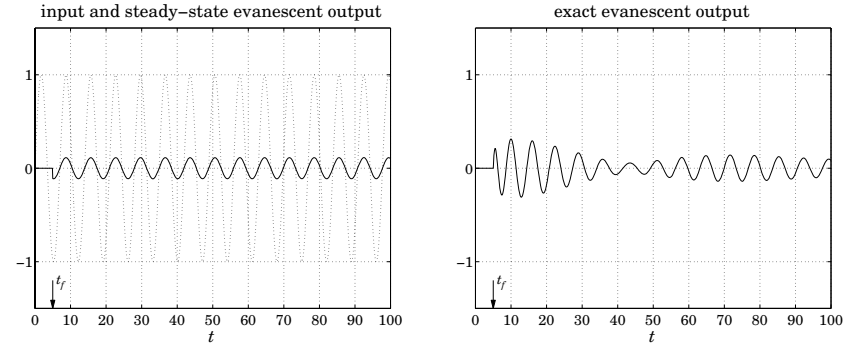
exact evanescent output

Fig. 3.4.2   Transient and steady-state response for evanescent sinusoids.

Fig. 3.4.2 illustrates an evanescent wave with $\omega_0 < \omega_p$. In this case the wavenumber becomes pure imaginary, $k_0 = -j\alpha_0 = -j\sqrt{\omega_p^2 - \omega_0^2}/c$, leading to an attenuated steady-state waveform:

$$E_{\text{steady}}(z,t) = e^{j\omega_0 t - jk_0 z} = e^{j\omega_0 t}e^{-\alpha_0 z}, \quad t \gg \frac{z}{c}$$

The following numerical values were used:

$$c = 1 \quad \omega_p = 1, \quad \omega_0 = 0.9, \quad t_f = z = 5$$

resulting in the imaginary wavenumber and attenuation amplitude:

$$k_0 = -j\alpha_0 = -0.4359j, \quad H_0 = e^{-jk_0 z} = e^{-\alpha_0 z} = 0.1131$$

We chose a smaller value of z in order to get a reasonable value for the attenuated signal for display purposes. The left graph in Fig. 3.4.2 shows the input and the steady-state output signals. The right graph shows the exact output computed by the same MATLAB code given above. Again, we note that for large t (here, $t > 80$), the exact output approaches the steady one.

Finally, in Fig. 3.4.3 we illustrate the input-on and input-off transients for an input rectangular pulse of duration t_d, and for a causal gaussian pulse, that is,

$$E(0,t) = \sin(\omega_0 t)\left[u(t) - u(t - t_d)\right], \quad E(0,t) = e^{j\omega_0 t}\exp\left[-\frac{(t - t_c)^2}{2\tau_0^2}\right]u(t)$$

The input-off transients for the rectangular pulse are due to the oscillating and decaying tail of the impulse response $h(z,t)$ given in (3.3.9). The following values of the parameters were used:

$$c = 1 \quad \omega_p = 1, \quad \omega_0 = 3, \quad t_f = z = 30, \quad t_d = 20, \quad t_c = \tau_0 = 5$$
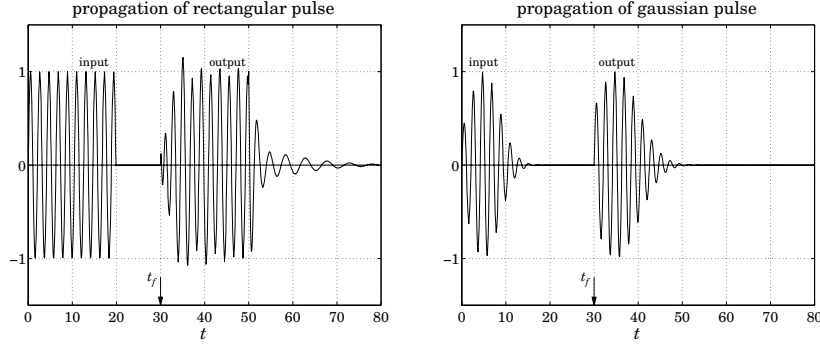
Fig. 3.4.3 Rectangular and gaussian pulse propagation.

The MATLAB code for the rectangular pulse case is essentially the same as above except that it uses the function upulse to enforce the finite pulse duration:

```
wp = 1; w0 = 3; tf = 30; td = 20; N = 15; K = 20;
k0 = -j * sqrt(j*(w0+wp)) * sqrt(j*(w0-wp));

t = linspace(0,80,801);

E0 = exp(j*w0*t) .* upulse(t,td);

for i=1:length(t),
  if t(i)<tf,
    Ez(i) = 0;
  else
    [w,x] = quadrs(linspace(tf,t(i),K), N);
    h = - wp^2 * tf * J1over(wp*sqrt(x.^2-tf^2)) .* ...
            exp(j*w0*(t(i)-x)) .* upulse(t(i)-x,td);
    Ez(i) = exp(j*w0*(t(i)-tf)).*upulse(t(i)-tf,td) + w'*h;
  end
end

e0 = imag(E0); ez = imag(Ez);

plot(t,ez,'-', t,e0,'-');
```

3.5 Pulse Propagation and Group Velocity

In this section, we show that the peak of a pulse travels with the group velocity. The concept of group velocity is associated with narrow-band pulses whose spectrum $\hat{E}(0,\omega)$ is narrowly concentrated in the neighborhood of some frequency, say, ω_0, with an effective frequency band $|\omega - \omega_0| \leq \Delta\omega$, where $\Delta\omega \ll \omega_0$, as depicted in Fig. 3.5.1.

Such spectrum can be made up by translating a low-frequency spectrum, say $\hat{F}(0,\omega)$, to ω_0, that is, $\hat{E}(0,\omega) = \hat{F}(0,\omega - \omega_0)$. From the modulation property of Fourier trans-
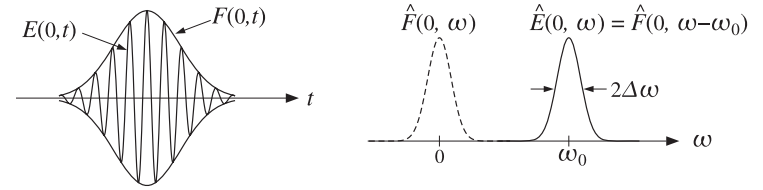
Fig. 3.5.1 High-frequency sinusoid with slowly-varying envelope.

forms, it follows that the corresponding time-domain signal $E(0,t)$ will be:

$$\hat{E}(0,\omega) = \hat{F}(0,\omega - \omega_0) \quad \Rightarrow \quad \boxed{E(0,t) = e^{j\omega_0 t}F(0,t)} \tag{3.5.1}$$

that is, a sinusoidal carrier modulated by a slowly varying envelope $F(0,t)$, where

$$F(0,t) = \frac{1}{2\pi}\int_{-\infty}^{\infty} e^{j\omega' t}\hat{F}(0,\omega')d\omega' = \frac{1}{2\pi}\int_{-\infty}^{\infty} e^{j(\omega-\omega_0)t}\hat{F}(0,\omega - \omega_0)d\omega \tag{3.5.2}$$

Because the integral over $\omega' = \omega - \omega_0$ is effectively restricted over the low-frequency band $|\omega'| \leq \Delta\omega$, the resulting envelope $F(0,t)$ will be slowly-varying (relative to the period $2\pi/\omega_0$ of the carrier.) If this pulse is launched into a dispersive medium with wavenumber $k(\omega)$, the propagated pulse to distance z will be given by:

$$E(z,t) = \frac{1}{2\pi}\int_{-\infty}^{\infty} e^{j(\omega t - kz)}\hat{F}(0,\omega - \omega_0)d\omega \tag{3.5.3}$$

Defining $k_0 = k(\omega_0)$, we may rewrite $E(z,t)$ in the form of a modulated plane wave:

$$\boxed{E(z,t) = e^{j(\omega_0 t - k_0 z)}F(z,t)} \tag{3.5.4}$$

where the propagated envelope $F(z,t)$ is given by

$$\boxed{F(z,t) = \frac{1}{2\pi}\int_{-\infty}^{\infty} e^{j(\omega-\omega_0)t - j(k-k_0)z}\hat{F}(0,\omega - \omega_0)d\omega} \tag{3.5.5}$$

This can also be written in a convolutional form by defining the *envelope impulse response* function $g(z,t)$ in terms of the propagator impulse response $h(z,t)$:

$$h(z,t) = e^{j(\omega_0 t - k_0 z)}g(z,t) \tag{3.5.6}$$

so that

$$g(z,t) = \frac{1}{2\pi}\int_{-\infty}^{\infty} e^{j(\omega-\omega_0)t - j(k-k_0)z}\,d\omega \tag{3.5.7}$$

Then, the propagated envelope can be obtained by the convolutional operation:

$$F(z,t) = \int_{-\infty}^{\infty} g(z,t')F(0,t - t')dt' \tag{3.5.8}$$

Because $\hat{F}(0, \omega - \omega_0)$ restricts the effective range of integration in Eq. (3.5.5) to a narrow band about ω_0, one can expand $k(\omega)$ to a Taylor series about ω_0 and keep only the first few terms:

$$k(\omega) = k_0 + k_0'(\omega - \omega_0) + \frac{1}{2}k_0''(\omega - \omega_0)^2 + \cdots \qquad (3.5.9)$$

where

$$k_0 = k(\omega_0), \quad k_0' = \frac{dk}{d\omega}\bigg|_{\omega_0}, \quad k_0'' = \frac{d^2k}{d\omega^2}\bigg|_{\omega_0} \qquad (3.5.10)$$

If $k(\omega)$ is real, we recognize k_0' as the inverse of the group velocity at frequency ω_0:

$$k_0' = \frac{dk}{d\omega}\bigg|_{\omega_0} = \frac{1}{v_g} \qquad (3.5.11)$$

If k_0' is complex-valued, $k_0' = \beta_0' - j\alpha_0'$, then its real part determines the group velocity through $\beta_0' = 1/v_g$, or, $v_g = 1/\beta_0'$. The second derivative k_0'' is referred to as the "dispersion coefficient" and is responsible for the spreading and chirping of the wave packet, as we see below.

Keeping up to the quadratic term in the quantity $k(\omega) - k_0$ in (3.5.5), and changing integration variables to $\omega' = \omega - \omega_0$, we obtain the approximation:

$$F(z, t) = \frac{1}{2\pi}\int_{-\infty}^{\infty} e^{j\omega'(t - k_0'z) - jk_0''z\omega'^2/2}\hat{F}(0, \omega')\, d\omega' \qquad (3.5.12)$$

In the *linear* approximation, we may keep k_0' and ignore the k_0'' term, and in the *quadratic* approximation, we keep both k_0' and k_0''. For the linear case, we have by comparing with Eq. (3.5.2):

$$F(z, t) = \frac{1}{2\pi}\int_{-\infty}^{\infty} e^{j\omega'(t - k_0'z)}\hat{F}(0, \omega')\, d\omega' = F(0, t - k_0'z) \qquad (3.5.13)$$

Thus, assuming that k_0' is real so that $k_0' = 1/v_g$, Eq. (3.5.13) implies that the initial envelope $F(0, t)$ is moving as whole with the group velocity v_g. The field $E(z, t)$ is obtained by modulating the high-frequency plane wave $e^{j(\omega_0 t - k_0 z)}$ with this envelope:

$$E(z, t) = e^{j(\omega_0 t - k_0 z)}F(0, t - z/v_g) \qquad (3.5.14)$$

Every point on the envelope travels at the same speed v_g, that is, its shape remains unchanged as it propagates, as shown in Fig. 3.5.2. The high-frequency carrier suffers a phase-shift given by $-k_0 z$.

Similar approximations can be introduced in (3.5.7) anticipating that (3.5.8) will be applied only to narrowband input envelope signals $F(0, t)$:

$$g(z, t) = \frac{1}{2\pi}\int_{-\infty}^{\infty} e^{j\omega'(t - k_0'z) - jk_0''z\omega'^2/2}\, d\omega' \qquad (3.5.15)$$

This integral can be done exactly, and leads to the following expressions in the linear and quadratic approximation cases (assuming that k_0', k_0'' are real):

linear:　　　　$g(z, t) = \delta(t - k_0'z)$

quadratic:　　$g(z, t) = \dfrac{1}{\sqrt{2\pi jk_0''z}}\exp\left[-\dfrac{(t - k_0'z)^2}{2jk_0''z}\right] \qquad (3.5.16)$
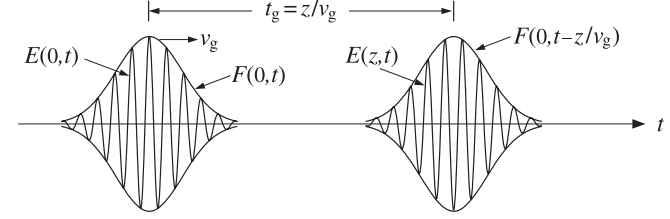
Fig. 3.5.2 Pulse envelope propagates with velocity v_g remaining unchanged in shape.

The corresponding frequency responses follow from Eq. (3.5.15), replacing ω' by ω:

linear:　　　　$G(z, \omega) = e^{-jk_0'z\omega}$

quadratic:　　$G(z, \omega) = e^{-jk_0'z\omega}e^{-jk_0''z\omega^2/2}$

$$(3.5.17)$$

The linear case is obtained from the quadratic one in the limit $k_0'' \to 0$. We note that the integral of Eq. (3.5.15), as well as the gaussian pulse examples that we consider later, are special cases of the following Fourier integral:

$$\frac{1}{2\pi}\int_{-\infty}^{\infty} e^{j\omega t - (a + jb)\omega^2/2}\, d\omega = \frac{1}{\sqrt{2\pi(a + jb)}}\exp\left[-\frac{t^2}{2(a + jb)}\right] \qquad (3.5.18)$$

where a, b are real, with the restriction that $a \geq 0$.[†] The integral for $g(z, t)$ corresponds to the case $a = 0$ and $b = k_0''z$. Using (3.5.16) into (3.5.8), we obtain Eq. (3.5.13) in the linear case and the following convolutional expression in the quadratic one:

linear:　　　　$F(z, t) = F(0, t - k_0'z)$

quadratic:　　$F(z, t) = \displaystyle\int_{-\infty}^{\infty} \dfrac{1}{\sqrt{2\pi jk_0''z}}\exp\left[-\dfrac{(t' - k_0'z)^2}{2jk_0''z}\right]F(0, t - t')\, dt'$

$$(3.5.19)$$

and in the frequency domain:

linear:　　　　$\hat{F}(z, \omega) = G(z, \omega)\hat{F}(0, \omega) = e^{-jk_0'z\omega}\hat{F}(0, \omega)$

quadratic:　　$\hat{F}(z, \omega) = G(z, \omega)\hat{F}(0, \omega) = e^{-jk_0'z\omega - jk_0''z\omega^2/2}\hat{F}(0, \omega)$

$$(3.5.20)$$

3.6 Group Velocity Dispersion and Pulse Spreading

In the linear approximation, the envelope propagates with the group velocity v_g, remaining unchanged in shape. But in the quadratic approximation, as a consequence of Eq. (3.5.19), it spreads and reduces in amplitude with distance z, and it chirps. To see this, consider a gaussian input pulse of effective width τ_0:

$$F(0, t) = \exp\left[-\frac{t^2}{2\tau_0^2}\right] \quad \Rightarrow \quad E(0, t) = e^{j\omega_0 t}F(0, t) = e^{j\omega_0 t}\exp\left[-\frac{t^2}{2\tau_0^2}\right] \qquad (3.6.1)$$

[†] Given the polar form $a + jb = Re^{j\theta}$, we must choose the square root $\sqrt{a + jb} = R^{1/2}e^{j\theta/2}$.

with Fourier transforms $\hat{F}(0, \omega)$ and $\hat{E}(0, \omega) = \hat{F}(0, \omega - \omega_0)$:

$$\hat{F}(0, \omega) = \sqrt{2\pi\tau_0^2}\, e^{-\tau_0^2 \omega^2/2} \quad \Rightarrow \quad \hat{E}(0, \omega) = \sqrt{2\pi\tau_0^2}\, e^{-\tau_0^2 (\omega - \omega_0)^2/2} \tag{3.6.2}$$

with an effective width $\Delta\omega = 1/\tau_0$. Thus, the condition $\Delta\omega \ll \omega_0$ requires that $\tau_0\omega_0 \gg 1$, that is, an envelope with a long duration relative to the carrier's period.

The propagated envelope $F(z, t)$ can be determined either from Eq. (3.5.19) or from (3.5.20). Using the latter, we have:

$$\hat{F}(z, \omega) = \sqrt{2\pi\tau_0^2}\, e^{-jk_0'z\omega - jk_0''z\omega^2/2} e^{-\tau_0^2 \omega^2/2} = \sqrt{2\pi\tau_0^2}\, e^{-jk_0'z\omega} e^{-(\tau_0^2 + jk_0''z)\omega^2/2} \tag{3.6.3}$$

The Fourier integral (3.5.18), then, gives the propagated envelope in the time domain:

$$F(z, t) = \sqrt{\frac{\tau_0^2}{\tau_0^2 + jk_0''z}} \exp\left[-\frac{(t - k_0'z)^2}{2(\tau_0^2 + jk_0''z)}\right] \tag{3.6.4}$$

Thus, effectively we have the replacement $\tau_0^2 \to \tau_0^2 + jk_0''z$. Assuming for the moment that k_0' and k_0'' are real, we find for the magnitude of the propagated pulse:

$$|F(z, t)| = \left[\frac{\tau_0^4}{\tau_0^4 + (k_0''z)^2}\right]^{1/4} \exp\left[-\frac{(t - k_0'z)^2 \tau_0^2}{2(\tau_0^4 + (k_0''z)^2)}\right] \tag{3.6.5}$$

where we used the property $|\tau_0^2 + jk_0''z| = \sqrt{\tau_0^4 + (k_0''z)^2}$. The effective width is determined from the argument of the exponent to be:

$$\tau^2 = \frac{\tau_0^4 + (k_0''z)^2}{\tau_0^2} \quad \Rightarrow \quad \tau = \left[\tau_0^2 + \left(\frac{k_0''z}{\tau_0}\right)^2\right]^{1/2} \tag{3.6.6}$$

Therefore, the pulse width increases with distance z. Also, the amplitude of the pulse decreases with distance, as measured for example at the peak maximum:

$$|F|_{\max} = \left[\frac{\tau_0^4}{\tau_0^4 + (k_0''z)^2}\right]^{1/4}$$

The peak maximum occurs at the group delay $t = k_0'z$, and hence it is moving at the group velocity $v_g = 1/k_0'$.

The effect of pulse spreading and amplitude reduction due to the term k_0'' is referred to as *group velocity dispersion* or *chromatic dispersion*. Fig. 3.6.1 shows the amplitude decrease and spreading of the pulse with distance, as well as the chirping effect (to be discussed in the next section.)

Because the frequency width is $\Delta\omega = 1/\tau_0$, we may write the excess time spread $\Delta\tau = k_0''z/\tau_0$ in the form $\Delta\tau = k_0''z\Delta\omega$. This can be understood in terms of the change in the group delay. It follows from $t_g = z/v_g = k'z$ that the change in t_g due to $\Delta\omega$ will be:

$$\Delta t_g = \frac{dt_g}{d\omega}\Delta\omega = \frac{dk'}{d\omega} z\Delta\omega = \frac{d^2k}{d\omega^2} z\Delta\omega = k''z\Delta\omega \tag{3.6.7}$$
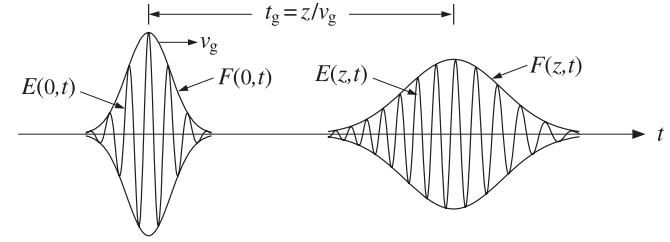
Fig. 3.6.1 Pulse spreading and chirping.

which can also be expressed in terms of the free-space wavelength $\lambda = 2\pi c/\omega$:

$$\Delta t_g = \frac{dt_g}{d\lambda}\Delta\lambda = \frac{dk'}{d\lambda} z\Delta\lambda = D z\Delta\lambda \tag{3.6.8}$$

where D is the "dispersion coefficient"

$$D = \frac{dk'}{d\lambda} = -\frac{2\pi c}{\lambda^2}\frac{dk'}{d\omega} = -\frac{2\pi c}{\lambda^2} k'' \tag{3.6.9}$$

where we replaced $d\lambda = -(\lambda^2/2\pi c)d\omega$. Since k' is related to the group refractive index n_g by $k' = 1/v_g = n_g/c$, we may obtain an alternative expression for D directly in terms of the refractive index n. Using Eq. (1.18.6), that is, $n_g = n - \lambda dn/d\lambda$, we find

$$D = \frac{dk'}{d\lambda} = \frac{1}{c}\frac{dn_g}{d\lambda} = \frac{1}{c}\frac{d}{d\lambda}\left[n - \lambda\frac{dn}{d\lambda}\right] = -\frac{\lambda}{c}\frac{d^2n}{d\lambda^2} \tag{3.6.10}$$

Combining Eqs. (3.6.9) and (3.6.10), we also have:

$$k'' = \frac{\lambda^3}{2\pi c^2}\frac{d^2n}{d\lambda^2} \tag{3.6.11}$$

In digital data transmission using optical fibers, the issue of pulse broadening as measured by (3.6.8) becomes important because it limits the maximum usable bit rate, or equivalently, the maximum propagation distance. The interpulse time interval of, say, T_b seconds by which bit pulses are separated corresponds to a data rate of $f_b = 1/T_b$ bits/second and must be longer than the broadening time, $T_b > \Delta t_g$, otherwise the broadened pulses will begin to overlap preventing their clear identification as separate. This limits the propagation distance z to a maximum value:[†]

$$D z\Delta\lambda \le T_b = \frac{1}{f_b} \quad \Rightarrow \quad \boxed{z \le \frac{1}{f_b D \Delta\lambda} = \frac{1}{f_b k''\Delta\omega}} \tag{3.6.12}$$

Because $D = \Delta t_g/z\Delta\lambda$, the parameter D is typically measured in units of picoseconds per km per nanometer—the km referring to the distance z and the nm to the wavelength spread $\Delta\lambda$. Similarly, the parameter $k'' = \Delta t_g/z\Delta\omega$ is measured in units of $\mathrm{ps}^2/\mathrm{km}$. As an example, we used the Sellmeier model for fused silica given in Eq. (1.11.16)
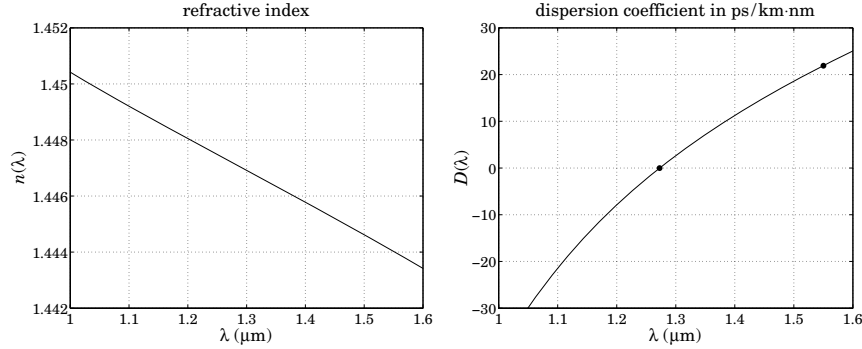
Fig. 3.6.2 Refractive index and dispersion coefficient of fused silica.

to plot in Fig. 3.6.2 the refractive index $n(\lambda)$ and the dispersion coefficient $D(\lambda)$ versus wavelength in the range $1 \leq \lambda \leq 1.6$ μm.

We observe that D vanishes, and hence also $k'' = 0$, at about $\lambda = 1.27$ μm corresponding to dispersionless propagation. This wavelength is referred to as a "zero dispersion wavelength." However, the preferred wavelength of operation is $\lambda = 1.55$ μm at which fiber losses are minimized. At $\lambda = 1.55$, we calculate the following refractive index values from the Sellmeier equation:

$$n = 1.444, \quad \frac{dn}{d\lambda} = -11.98 \times 10^{-3} \ \mu m^{-1}, \quad \frac{d^2 n}{d\lambda^2} = -4.24 \times 10^{-3} \ \mu m^{-2} \qquad (3.6.13)$$

resulting in the group index $n_g = 1.463$ and group velocity $v_g = c/n_g = 0.684c$. Using (3.6.10) and (3.6.11), the calculated values of D and k'' are:

$$D = 21.9 \ \frac{ps}{km \cdot nm}, \quad k'' = -27.9 \ \frac{ps^2}{km} \qquad (3.6.14)$$

The ITU-G.652 standard single-mode fiber [229] has the following nominal values of the dispersion parameters at $\lambda = 1.55$ μm:

$$D = 17 \ \frac{ps}{km \cdot nm}, \quad k'' = -21.67 \ \frac{ps^2}{km} \qquad (3.6.15)$$

with the dispersion coefficient $D(\lambda)$ given approximately by the fitted linearized form in the neighborhood of 1.55 μm:

$$D(\lambda) = 17 + 0.056 (\lambda - 1550) \ \frac{ps}{km \cdot nm}, \quad \text{with } \lambda \text{ in units of nm}$$

Moreover, the standard fiber has a zero-dispersion wavelength of about 1.31 μm and an attenuation constant of about 0.2 dB/km.

We can use the values in (3.6.15) to get a rough estimate of the maximum propagation distance in a standard fiber. We assume that the data rate is $f_b = 40$ Gbit/s, so that the

---

†where the absolute values of D, k'' must be used in Eq. (3.6.12).

interpulse spacing is $T_b = 25$ ps. For a 10 picosecond pulse, i.e., $\tau_0 = 10$ ps and $\Delta\omega = 1/\tau_0 = 0.1$ rad/ps, we estimate the wavelength spread to be $\Delta\lambda = (\lambda^2/2\pi c)\Delta\omega = 0.1275$ nm at $\lambda = 1.55$ μm. Using Eq. (3.6.12), we find the limit $z \leq 11.53$ km—a distance that falls short of the 40-km and 80-km recommended lengths.

Longer propagation lengths can be achieved by using dispersion compensation techniques, such as using chirped inputs or adding negative-dispersion fiber lengths. We discuss chirping and dispersion compensation in the next two sections.

The result (3.6.4) remains valid [186], with some caveats, when the wavenumber is complex valued, $k(\omega) = \beta(\omega) - j\alpha(\omega)$. The parameters $k_0' = \beta_0' - j\alpha_0'$ and $k_0'' = \beta_0'' - j\alpha_0''$ can be substituted in Eqs. (3.6.3) and (3.6.4):

$$\hat{F}(z, \omega) = \sqrt{2\pi\tau_0^2} \ e^{-j(\beta_0' - j\alpha_0')z\omega} \ e^{-\left(\tau_0^2 + (\alpha_0'' + j\beta_0'')z\right)\omega^2/2}$$

$$F(z, t) = \sqrt{\frac{\tau_0^2}{\tau_0^2 + \alpha_0'' z + j\beta_0'' z}} \ \exp\left[-\frac{(t - (\beta_0' - j\alpha_0')z)^2}{2(\tau_0^2 + \alpha_0'' z + j\beta_0'' z)}\right] \qquad (3.6.16)$$

The Fourier integral (3.5.18) requires that the real part of the effective complex width $\tau_0^2 + jk_0'' z = (\tau_0^2 + \alpha_0'' z) + j\beta_0'' z$ be positive, that is, $\tau_0^2 + \alpha_0'' z > 0$. If α_0'' is negative, this condition limits the distances z over which the above approximations are valid. The exponent can be written in the form:

$$-\frac{(t - (\beta_0' - j\alpha_0')z)^2}{2(\tau_0^2 + \alpha_0'' z + j\beta_0'' z)} = -\frac{(t - \beta_0' z + j\alpha_o' z)^2 (\tau_0^2 + \alpha_0'' z - j\beta_0'' z)}{2\left[(\tau_0^2 + \alpha_0'' z)^2 + (\beta_0'' z)^2\right]} \qquad (3.6.17)$$

Separating this into its real and imaginary parts, one can show after some algebra that the magnitude of $F(z, t)$ is given by:†

$$|F(z, t)| = \left[\frac{\tau_0^4}{(\tau_0^2 + \alpha_0'' z)^2 + (\beta_0'' z)^2}\right]^{1/4} \exp\left[\frac{\alpha_0'^2 z^2}{2(\tau_0^2 + \alpha_0'' z)}\right] \cdot \exp\left[-\frac{(t - t_g)^2}{2\tau^2}\right] \qquad (3.6.18)$$

where the peak of the pulse does not quite occur at the ordinary group delay $t_g = \beta_0' z$, but rather at the effective group delay:

$$t_g = \beta_0' z - \frac{\alpha_0' \beta_0'' z^2}{\tau_0^2 + \alpha_0'' z}$$

The effective width of the peak generalizes Eq. (3.6.6)

$$\tau^2 = \tau_0^2 + \alpha_0'' z + \frac{(\beta_0'' z)^2}{\tau_0^2 + \alpha_0'' z}$$

From the imaginary part of Eq. (3.6.17), we observe two additional effects. First, the non-zero coefficient of the jt term is equivalent to a z-dependent frequency shift of the carrier frequency ω_0, and second, from the coefficient of $jt^2/2$, there will be a certain amount of chirping as discussed in the next section. The frequency shift and chirping coefficient (generalizing Eq. (3.7.6)) turn out to be:

$$\Delta\omega_0 = -\frac{\alpha_o' z (\tau_0^2 + \alpha_0'' z)}{(\tau_0^2 + \alpha_0'' z)^2 + (\beta_0'' z)^2}, \quad \dot{\omega}_0 = \frac{\beta_0'' z}{(\tau_0^2 + \alpha_0'' z)^2 + (\beta_0'' z)^2}$$

---

†note that if $F = Ae^B$, then $|F| = |A|e^{\text{Re}(B)}$.

3.7 Propagation and Chirping

A chirped sinusoid has an instantaneous frequency that changes *linearly* with time, referred to as linear frequency modulation (FM). It is obtained by the substitution:

$$e^{j\omega_0 t} \quad \rightarrow \quad e^{j(\omega_0 t + \dot\omega_0 t^2/2)} \tag{3.7.1}$$

where the "chirping parameter" $\dot\omega_0$ is a constant representing the rate of change of the instantaneous frequency. The phase $\theta(t)$ and instantaneous frequency $\dot\theta(t) = d\theta(t)/dt$ are for the above sinusoids:

$$\begin{aligned} \theta(t) = \omega_0 t \quad &\rightarrow \quad \theta(t) = \omega_0 t + \frac{1}{2}\dot\omega_0 t^2 \\ \dot\theta(t) = \omega_0 \quad &\rightarrow \quad \dot\theta(t) = \omega_0 + \dot\omega_0 t \end{aligned} \tag{3.7.2}$$

The parameter $\dot\omega_0$ can be positive or negative resulting in an increasing or decreasing instantaneous frequency. A chirped gaussian pulse is obtained by modulating a chirped sinusoid by a gaussian envelope:

$$E(0,t) = e^{j(\omega_0 t + \dot\omega_0 t^2/2)} \exp\left[-\frac{t^2}{2\tau_0^2}\right] = e^{j\omega_0 t} \exp\left[-\frac{t^2}{2\tau_0^2}(1 - j\dot\omega_0 \tau_0^2)\right] \tag{3.7.3}$$

which can be written in the following form, in the time and frequency domains:

$$E(0,t) = e^{j\omega_0 t} \exp\left[-\frac{t^2}{2\tau_{\text{chirp}}^2}\right] \quad \Leftrightarrow \quad \hat E(0,\omega) = \sqrt{2\pi\tau_{\text{chirp}}^2}\, e^{-\tau_{\text{chirp}}^2(\omega - \omega_0)^2/2} \tag{3.7.4}$$

where τ_{chirp}^2 is an equivalent complex-valued width parameter defined by:

$$\tau_{\text{chirp}}^2 = \frac{\tau_0^2}{1 - j\dot\omega_0 \tau_0^2} = \frac{\tau_0^2(1 + j\dot\omega_0 \tau_0^2)}{1 + \dot\omega_0^2 \tau_0^4} \tag{3.7.5}$$

Thus, a complex-valued width is associated with linear chirping. An unchirped gaussian pulse that propagates by a distance z into a medium becomes chirped because it acquires a complex-valued width, that is, $\tau_0^2 + jk_0'' z$, as given by Eq. (3.6.4). Therefore, propagation is associated with chirping. Close inspection of Fig. 3.6.1 reveals that the front of the pulse appears to have a higher carrier frequency than its back (in this figure, we took $k_0'' < 0$, for normal dispersion). The effective chirping parameter $\dot\omega_0$ can be identified by writing the propagated envelope in the form:

$$\begin{aligned} F(z,t) &= \sqrt{\frac{\tau_0^2}{\tau_0^2 + jk_0'' z}} \exp\left[-\frac{(t - k_0' z)^2}{2(\tau_0^2 + jk_0'' z)}\right] \\ &= \sqrt{\frac{\tau_0^2}{\tau_0^2 + jk_0'' z}} \exp\left[-\frac{(t - k_0' z)^2}{2(\tau_0^4 + (k_0'' z)^2)}(\tau_0^2 - jk_0'' z)\right] \end{aligned}$$

Comparing with (3.7.3), we identify the chirping parameter due to propagation:

$$\dot\omega_0 = \frac{k_0'' z}{\tau_0^4 + (k_0'' z)^2} \tag{3.7.6}$$

If a *chirped gaussian input* is launched into a propagation medium, then the chirping due to propagation will combine with the input chirping. The two effects can sometimes cancel each other leading to *pulse compression* rather than spreading. Indeed, if the chirped pulse (3.7.4) is propagated by a distance z, then according to (3.6.4), the propagated envelope will be:

$$F(z,t) = \sqrt{\frac{\tau_{\text{chirp}}^2}{\tau_{\text{chirp}}^2 + jk_0'' z}} \exp\left[-\frac{(t - k_0' z)^2}{2(\tau_{\text{chirp}}^2 + jk_0'' z)}\right] \tag{3.7.7}$$

The effective complex-valued width parameter will be:

$$\tau_{\text{chirp}}^2 + jk_0'' z = \frac{\tau_0^2(1 + j\dot\omega_0 \tau_0^2)}{1 + \dot\omega_0^2 \tau_0^4} + jk_0'' z = \frac{\tau_0^2}{1 + \dot\omega_0^2 \tau_0^4} + j\left(\frac{\dot\omega_0 \tau_0^4}{1 + \dot\omega_0^2 \tau_0^4} + k_0'' z\right) \tag{3.7.8}$$

If $\dot\omega_0$ is selected such that

$$\frac{\dot\omega_0 \tau_0^4}{1 + \dot\omega_0^2 \tau_0^4} = -k_0'' z_0$$

for some positive distance z_0, then the effective width (3.7.8) can be written as:

$$\tau_{\text{chirp}}^2 + jk_0'' z = \frac{\tau_0^2}{1 + \dot\omega_0^2 \tau_0^4} + jk_0''(z - z_0) \tag{3.7.9}$$

and as z increases over the interval $0 \le z \le z_0$, the pulse width will be getting narrower, becoming the narrowest at $z = z_0$. Beyond, $z > z_0$, the pulse width will start increasing again. Thus, the initial chirping and the chirping due to propagation cancel each other at $z = z_0$. Some dispersion compensation methods are based on this effect.

3.8 Dispersion Compensation

The filtering effect of the propagation medium is represented in the frequency domain by $\hat F(z,\omega) = G(z,\omega)\hat F(0,\omega)$, where the transfer function $G(z,\omega)$ is given by Eq. (3.5.20).

To counteract the effect of spreading, a compensation filter $H_{\text{comp}}(\omega)$ may be inserted at the end of the propagation medium as shown in Fig. 3.8.1 that effectively equalizes the propagation response, up to a prescribed delay t_d, that is,

$$G(z,\omega) H_{\text{comp}}(\omega) = e^{-j\omega t_d} \quad \Rightarrow \quad \boxed{H_{\text{comp}}(\omega) = \frac{e^{-j\omega t_d}}{G(z,\omega)}} \tag{3.8.1}$$

The overall compensated output will be the input delayed by t_d, that is, $F_{\text{comp}}(z,t) = F(0, t - t_d)$. For example, if the delay is chosen to be the group delay $t_d = t_g = k_0' z$, then, in the quadratic approximation for $G(z,\omega)$, condition (3.8.1) reads:

$$G(z,\omega) H_{\text{comp}}(\omega) = e^{-jk_0' z\omega} e^{-jk_0'' z\omega^2/2} H_{\text{comp}}(\omega) = e^{-jk_0' z\omega}$$
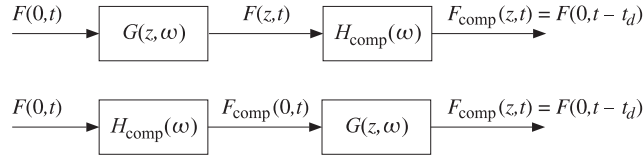
Fig. 3.8.1 Dispersion compensation filters.

which gives for the compensation filter:

$$H_{\text{comp}}(\omega) = e^{jk_0'' z \omega^2/2} \tag{3.8.2}$$

with impulse response:

$$h_{\text{comp}}(t) = \frac{1}{\sqrt{-2\pi jk_0'' z}} \exp\left[\frac{t^2}{2jk_0'' z}\right] \tag{3.8.3}$$

The output of the compensation filter will then agree with that of the linear approximation case, that is, it will be the input delayed as a whole by the group delay:

$$F_{\text{comp}}(z,\omega) = H_{\text{comp}}(\omega)\hat{F}(z,\omega) = H_{\text{comp}}(\omega)G(z,\omega)\hat{F}(0,\omega) = e^{-jk_0' z \omega}\hat{F}(0,\omega)$$

or, in the time domain, $F_{\text{comp}}(z,t) = F(0, t - k_0' z)$.

As shown in Fig. 3.8.1, it is possible [221] to insert the compensation filter at the input end. The pre-compensated input then suffers an equal and opposite dispersion as it propagates by a distance z, resulting in the same compensated output. As an example, an input gaussian and its pre-compensated version will be:

$$\hat{F}(0,\omega) = \sqrt{2\pi\tau_0^2}\, e^{-\tau_0^2 \omega^2/2}, \quad \hat{F}_{\text{comp}}(0,\omega) = H_{\text{comp}}(\omega)\hat{F}(0,\omega) = \sqrt{2\pi\tau_0^2}\, e^{-(\tau_0^2 - jk_0'' z)\omega^2/2}$$

and in the time domain:

$$F(0,t) = \exp\left[-\frac{t^2}{2\tau_0^2}\right], \quad F_{\text{comp}}(0,t) = \sqrt{\frac{\tau_0^2}{\tau_0^2 - jk_0'' z}} \exp\left[-\frac{t^2}{2(\tau_0^2 - jk_0'' z)}\right]$$

This corresponds to a chirped gaussian input with a chirping parameter opposite that of Eq. (3.7.6). If the pre-compensated signal is propagated by a distance z, then its new complex-width will be, $(\tau_0^2 - jk_0'' z) + jk_0'' z = \tau_0^2$, and its new amplitude:

$$\sqrt{\frac{\tau_0^2}{\tau_0^2 - jk_0'' z}} \sqrt{\frac{\tau_0^2 - jk_0'' z}{(\tau_0^2 - jk_0'' z) + jk_0'' z}} = 1$$

thus, including the group delay, the propagated signal will be $F_{\text{comp}}(z,t) = F(0, t - k_0' z)$.

There are many ways of implementing dispersion compensation filters in optical fiber applications, such as using appropriately chirped inputs, or using fiber delay-line filters at either end, or appending a length of fiber that has equal end opposite dispersion. The latter method is one of the most widely used and is depicted below:
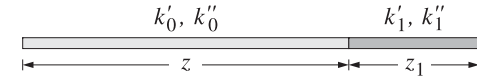
To see how it works, let the appended fiber have length z_1 and group delay and dispersion parameters k_1', k_1''. Then, its transfer function will be:

$$G_1(z_1, \omega) = e^{-jk_1' z_1 \omega} e^{-jk_1'' z_1 \omega^2/2}$$

The combined transfer function of propagating through the main fiber of length z followed by z_1 will be:

$$\begin{aligned} G(z,\omega)G_1(z_1,\omega) &= e^{-jk_0' z \omega} e^{-jk_0'' z \omega^2/2} e^{-jk_1' z_1 \omega} e^{-jk_1'' z_1 \omega^2/2} \\ &= e^{-j(k_0' z + k_1' z_1)\omega} e^{-j(k_0'' z + k_1'' z_1)\omega^2/2} \end{aligned} \tag{3.8.4}$$

If k_1'' has the opposite sign from k_0'' and z_1 is chosen such that $k_0'' z + k_1'' z_1 = 0$, or, $k_1'' z_1 = -k_0'' z$, then the dispersion will be canceled. Thus, up to a delay, $G_1(z_1, \omega)$ acts just like the required compensation filter $H_{\text{comp}}(\omega)$. In practice, the appended fiber is manufactured to have $|k_1''| \gg |k_0''|$, so that its length will be short, $z_1 = -k_0'' z/k_1'' \ll z$.

3.9 Slow, Fast, and Negative Group Velocities

The group velocity approximations of Sec. 3.5 are valid when the signal band is narrowly centered about a carrier frequency ω_0 around which the wavenumber $k(\omega)$ is a slowly-varying function of frequency to justify the Taylor series expansion (3.5.9).

The approximations are of questionable validity in spectral regions where the wavenumber, or equivalently, the refractive index $n(\omega)$, are varying rapidly with frequency, such as in the immediate vicinity of absorption or gain resonances in the propagation medium. However, even in such cases, the basic group velocity approximation, $F(z,t) = F(0, t - z/v_g)$, can be justified provided the signal bandwidth $\Delta\omega$ is sufficiently narrow and the propagation distance z is sufficiently short to minimize spreading and chirping; for example, in the gaussian case, this would require the condition $|k_0'' z| \ll \tau_0^2$, or, $|k_0'' z(\Delta\omega)^2| \ll 1$, as well as the condition $|\text{Im}(k_0)z| \ll 1$ to minimize amplitude distortions due to absorption or gain.

Because near resonances the group velocity v_g can be subluminal, superluminal, or negative, this raises the issue of how to interpret the result $F(z,t) = F(0, t - z/v_g)$. For example, if v_g is negative within a medium of thickness z, then the group delay $t_g = z/v_g$ will be negative, corresponding to a *time advance*, and the envelope's peak will appear to exit the medium before it even enters it. Indeed, experiments have demonstrated such apparently bizarre behavior [251,252,270]. As we mentioned in Sec. 3.2, this is not at odds with relativistic causality because the peaks are not necessarily causally related—only sharp signal fronts may not travel faster than c.

The gaussian pulses used in the above experiments do not have a sharp front. Their (infinitely long) forward tail can enter and exit the medium well before the peak does. Because of the spectral reshaping taking place due to the propagation medium's response $e^{-jk(\omega)z}$, the forward portion of the pulse that is already within the propagation

medium, and the portion that has already exited, can get reshaped into a peak that appears to have exited before the peak of the input has entered. In fact, before the incident peak enters the medium, two additional peaks develop caused by the forward tail of the input: the one that has already exited the medium, and another one within the medium traveling *backwards* with the negative group velocity v_g. Such backward-moving peaks have been observed experimentally [298]. We clarify these remarks later on by means of the numerical example shown in Fig. 3.9.4 and elaborated further in Problem 3.10.

Next, we look at some examples that are good candidates for demonstrating the above ideas. We recall from Sec. 1.18 the following relationships between wavenumber $k = \beta - j\alpha$, refractive index $n = n_r - jn_i$, group index n_g, and dispersion coefficient k'', where all the quantities are functions of the frequency ω:

$$k = \beta - j\alpha = \frac{\omega n}{c} = \frac{\omega(n_r - jn_i)}{c}$$

$$k' = \frac{dk}{d\omega} = \frac{1}{c}\frac{d(\omega n)}{d\omega} = \frac{n_g}{c} \quad \Rightarrow \quad v_g = \frac{1}{\mathrm{Re}(k')} = \frac{c}{\mathrm{Re}(n_g)} \tag{3.9.1}$$

$$k'' = \frac{d^2 k}{d\omega^2} = \frac{1}{c}\frac{dn_g}{d\omega} = \frac{n_g'}{c}$$

We consider first a single-resonance absorption or gain Lorentz medium with permittivity given by Eq. (1.11.13), that is, having susceptibility χ and refractive index n:

$$\chi = \frac{f\omega_p^2}{\omega_r^2 - \omega^2 + j\omega\gamma} \quad \Rightarrow \quad n = \sqrt{1 + \chi} = \sqrt{1 + \frac{f\omega_p^2}{\omega_r^2 - \omega^2 + j\omega\gamma}} \tag{3.9.2}$$

where ω_r, γ are the resonance frequency and linewidth, and ω_p, f are the plasma frequency and oscillator strength. For an absorption medium, we will set $f = 1$, for a gain medium, $f = -1$, and for vacuum, $f = 0$. To simplify the algebra, we may use the approximation (1.18.3), that is,

$$n = \sqrt{1 + \chi} \simeq 1 + \frac{1}{2}\chi = 1 + \frac{f\omega_p^2/2}{\omega_r^2 - \omega^2 + j\omega\gamma} \tag{3.9.3}$$

This approximation is fairly accurate in the numerical examples that we consider. The corresponding complex-valued group index follows from (3.9.3):

$$n_g = \frac{d(\omega n)}{d\omega} = 1 + \frac{f\omega_p^2(\omega^2 + \omega_r^2)/2}{(\omega_r^2 - \omega^2 + j\omega\gamma)^2} \tag{3.9.4}$$

with real and imaginary parts:

$$\mathrm{Re}(n_g) = 1 + \frac{f\omega_p^2(\omega^2 + \omega_r^2)\left[(\omega^2 - \omega_r^2)^2 - \omega^2\gamma^2\right]}{\left[(\omega^2 - \omega_r^2)^2 + \omega^2\gamma^2\right]^2}$$

$$\mathrm{Im}(n_g) = \frac{f\omega_p^2\gamma\omega(\omega^4 - \omega_r^4)}{\left[(\omega^2 - \omega_r^2)^2 + \omega^2\gamma^2\right]^2} \tag{3.9.5}$$

Similarly, the dispersion coefficient $dn_g/d\omega$ is given by:

$$n_g' = \frac{dn_g}{d\omega} = \frac{f\omega_p^2(\omega^3 + 3\omega_r^2\omega - j\gamma\omega_r^2)}{(\omega_r^2 - \omega^2 + j\omega\gamma)^3} \tag{3.9.6}$$

At resonance, $\omega = \omega_r$, we find the values:

$$n = 1 - j\frac{f\omega_p^2}{2\gamma\omega_r}, \quad n_g = 1 - \frac{f\omega_p^2}{\gamma^2} \tag{3.9.7}$$

For an absorption medium ($f = 1$), if $\omega_p < \gamma$, the group index will be $0 < n_g < 1$, resulting into a superluminal group velocity $v_g = c/n_g > c$, but if $\gamma < \omega_p$, which is the more typical case, then the group index will become negative, resulting into a negative $v_g = c/n_g < 0$. This is illustrated in the top row of graphs of Fig. 3.9.1. On the other hand, for a gain medium ($f = -1$), the group index is always $n_g > 1$ at resonance, resulting into a subluminal group velocity $v_g = c/n_g < c$. This is illustrated in the middle and bottom rows of graphs of Fig. 3.9.1.
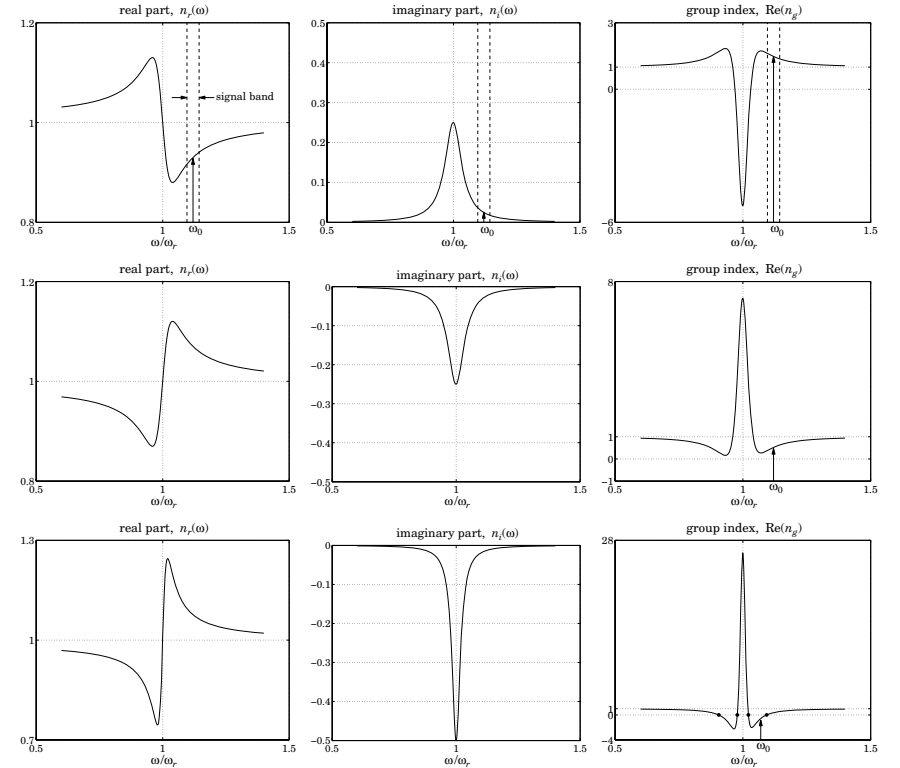

Fig. 3.9.1 Slow, fast, and negative group velocities (at off resonance).

Fig. 3.9.1 plots $n(\omega) = n_r(\omega) - jn_i(\omega)$ and $\mathrm{Re}[n_g(\omega)]$ versus ω, evaluated using Eqs. (3.9.3) and (3.9.4), with the frequency axis normalized in units of ω/ω_r. The

following values of the parameters were used (with arbitrary frequency units):

$$\begin{aligned}
\text{(top row)} \quad & f = +1\,, \quad \omega_p = 1\,, \quad \omega_r = 5\,, \quad \gamma = 0.4 \\
\text{(middle row)} \quad & f = -1\,, \quad \omega_p = 1\,, \quad \omega_r = 5\,, \quad \gamma = 0.4 \\
\text{(bottom row)} \quad & f = -1\,, \quad \omega_p = 1\,, \quad \omega_r = 5\,, \quad \gamma = 0.2
\end{aligned}$$

The calculated values of n, n_g at resonance were:

$$\begin{aligned}
\text{(top)} \quad & \omega = \omega_r\,, \quad n = 1 - 0.25j\,, \quad n_g = -5.25 \\
\text{(middle)} \quad & \omega = \omega_r\,, \quad n = 1 + 0.25j\,, \quad n_g = 7.25 \\
\text{(bottom)} \quad & \omega = \omega_r\,, \quad n = 1 + 0.5j\,, \quad n_g = 26
\end{aligned}$$

Operating at resonance is not a good idea because of the fairly substantial amounts of attenuation or gain arising from the imaginary part n_i of the refractive index, which would cause amplitude distortions in the signal as it propagates.

A better operating frequency band is at off resonance where the attenuation or gain are lower [257]. The top row of Fig. 3.9.1 shows such a band centered at a frequency ω_0 on the right wing of the resonance, with a narrow enough bandwidth to justify the Taylor series expansion (3.5.9). The group velocity behavior is essentially the reverse of that at resonance, that is, v_g becomes subluminal for the absorption medium, and superluminal or negative for the gain medium. The carrier frequency ω_0 and the calculated values of n, n_g at $\omega = \omega_0$ were as follows:

$$\begin{aligned}
\text{(top, slow)} \quad & \omega_0/\omega_r = 1.12\,, \quad n = 0.93 - 0.02j\,, \quad n_g = 1.48 + 0.39j \\
\text{(middle, fast)} \quad & \omega_0/\omega_r = 1.12\,, \quad n = 1.07 + 0.02j\,, \quad n_g = 0.52 - 0.39j \\
\text{(bottom, negative)} \quad & \omega_0/\omega_r = 1.07\,, \quad n = 1.13 + 0.04j\,, \quad n_g = -0.58 - 1.02j
\end{aligned}$$

We note the sign and magnitude of $\mathrm{Re}(n_g)$ and the substantially smaller values of the imaginary part n_i. For the middle graph, the group index remains in the interval $0 < \mathrm{Re}(n_g) < 1$, and hence $v_g > c$, for all values of the frequency in the right wing of the resonance.

In order to get negative values for $\mathrm{Re}(n_g)$ and for v_g, the linewidth γ must be reduced. As can be seen in the bottom row of graphs, $\mathrm{Re}(n_g)$ becomes negative over a small range of frequencies to the right and left of the resonance. The edge frequencies can be calculated from the zero-crossings of $\mathrm{Re}(n_g)$ and are shown on the graph. For the given parameter values, they were found to be (in units of ω/ω_r):

$$[0.9058, 0.9784]\,, \quad [1.0221, 1.0928]$$

The chosen value of $\omega_0/\omega_r = 1.07$ falls inside the right interval.

Another way of demonstrating slow, fast, or negative group velocities with low attenuation or gain, which has been used in practice, is to operate at a frequency band that lies between two nearby absorption or gain lines.

Some examples are shown in Fig. 3.9.2. The top row of graphs depicts the case of two nearby absorption lines. In the band between the lines, the refractive index exhibits normal dispersion. Exactly at midpoint, the attenuation is minimal and the real part n_r has a steep slope that causes a large group index, $\mathrm{Re}(n_g) \gg 1$, and hence a small positive group velocity $0 < v_g \ll c$. In experiments, very sharp slopes have been
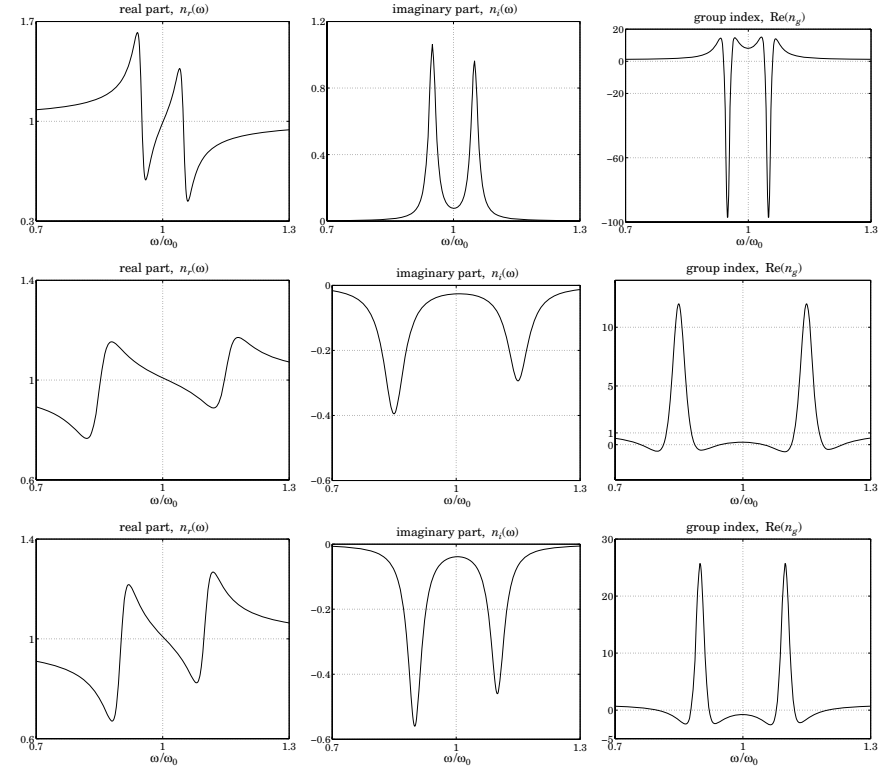
Fig. 3.9.2 Slow, fast, and negative group velocities (halfway between resonances).

achieved through the use of the so-called "electromagnetically induced transparency," resulting into extremely slow group velocities of the order of tens of m/sec [312].

The middle row of graphs depicts two nearby gain lines [258] with a small gain at midpoint and a real part n_r that has a negative slope resulting into a group index $0 < \mathrm{Re}(n_g) < 1$, and a superluminal group velocity $v_g > c$.

Choosing more closely separated peaks in the third row of graphs, has the effect of increasing the negative slope of n_r, thus causing the group index to become negative at midpoint, $\mathrm{Re}(n_g) < 0$, resulting in negative group velocity, $v_g < 0$. Experiments demonstrating this behavior have received a lot of attention [270].

The following expressions were used in Fig. 3.9.2 for the refractive and group indices,

with $f = 1$ for the absorption case, and $f = -1$ for the gain case:

$$n = 1 + \frac{f\omega_p^2/2}{\omega_1^2 - \omega^2 + j\omega\gamma} + \frac{f\omega_p^2/2}{\omega_2^2 - \omega^2 + j\omega\gamma}$$

$$n_g = 1 + \frac{f\omega_p^2(\omega^2 + \omega_1^2)/2}{(\omega_1^2 - \omega^2 + j\omega\gamma)^2} + \frac{f\omega_p^2(\omega^2 + \omega_2^2)/2}{(\omega_2^2 - \omega^2 + j\omega\gamma)^2} \tag{3.9.8}$$

The two peaks were symmetrically placed about the midpoint frequency ω_0, that is, at $\omega_1 = \omega_0 - \Delta$ and $\omega_2 = \omega_0 + \Delta$, and a common linewidth γ was chosen. The particular numerical values used in this graph were:

(top, slow)	$f = +1$,	$\omega_p = 1$,	$\omega_0 = 5$,	$\Delta = 0.25$,	$\gamma = 0.1$
(middle, fast)	$f = -1$,	$\omega_p = 1$,	$\omega_0 = 5$,	$\Delta = 0.75$,	$\gamma = 0.3$
(bottom, negative)	$f = -1$,	$\omega_p = 1$,	$\omega_0 = 5$,	$\Delta = 0.50$,	$\gamma = 0.2$

resulting in the following values for n and n_g:

(top, slow)	$n = 0.991 - 0.077j$,	$n_g = 8.104 + 0.063j$
(middle, fast)	$n = 1.009 + 0.026j$,	$n_g = 0.208 - 0.021j$
(bottom, negative)	$n = 1.009 + 0.039j$,	$n_g = -0.778 - 0.032j$

Next, we look at an example of a gaussian pulse propagating through a medium with negative group velocity. We consider a single-resonance gain medium and operating frequency band similar to that shown in the bottom row of graphs in Fig. 3.9.1. This example is variation of that discussed in [257]. Fig. 3.9.3 shows the geometry.
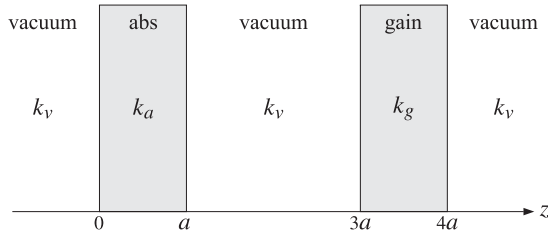

Fig. 3.9.3 Absorption and gain media separated by vacuum.

The gaussian pulse begins in vacuum on the left, then it enters an absorbing medium of thickness a in which it propagates with a slow group velocity suffering a modest amount of attenuation. It then enters a vacuum region of width $2a$, followed by a gain medium of thickness a in which it propagates with negative group velocity suffering a moderate amount gain, and finally it exits into vacuum.

The attenuation and gain are adjusted to compensate each other, so that the final output vacuum pulse is identical to the input.

The wavenumbers k_v, k_a, k_g, in vacuum, the absorption and gain media are calculated from Eqs. (3.9.1)–(3.9.6) with $f = 0, +1, -1$, respectively. The analytical and
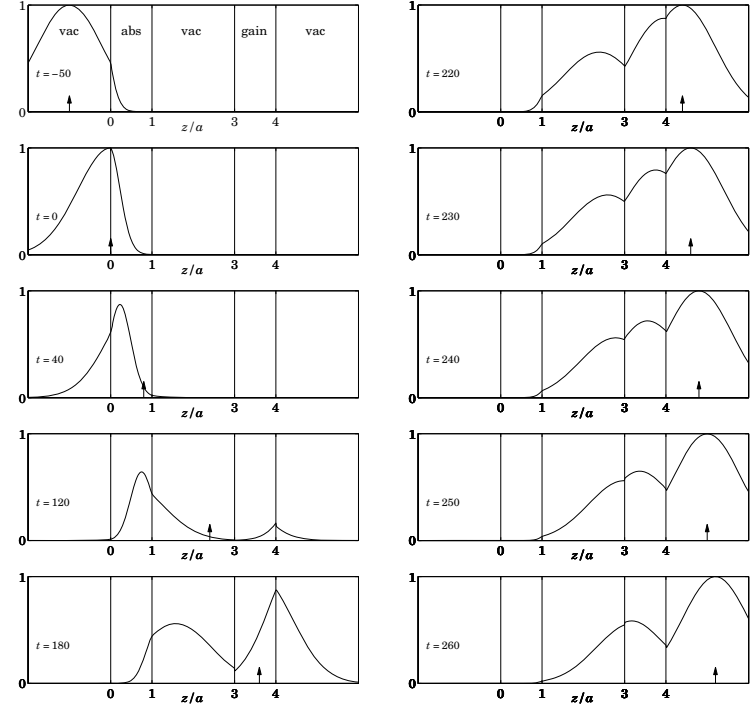

Fig. 3.9.4 Snapshots of pulse propagating through regions of different group velocities.

numerical details for this example are outlined in Problem 3.10. Fig. 3.9.4 shows a series of snapshots. The short vertical arrow on the horizontal axis represents the position of the peak of an equivalent pulse propagating in vacuum.

At $t = -50$ (in units such that $c = 1$), the forward tail of the gaussian pulse has already entered the absorbing medium. Between $0 \le t \le 120$, the peak of the pulse has entered the absorbing medium and is being attenuated as it propagates while it lags behind the equivalent vacuum pulse because $v_g < c$.

At $t = 120$, while the peak is still in the absorbing medium, the forward tail has passed through the middle vacuum region and has already entered into the gain medium where it begins to get amplified. At $t = 180$, the peak has moved into the middle vacuum region, but the forward tail has been sufficiently amplified by the gain medium and is beginning to form a peak whose tail has already exited into the rightmost vacuum region.

At $t = 220$, the peak is still within the middle vacuum region, but the output peak has already exited into the right, while another peak has formed at the right side of the gain medium and begins to move backwards with the negative group velocity, $v_g < 0$. Meanwhile, the output peak has caught up with the equivalent vacuum peak.

Between $230 \le t \le 260$, the peak within the gain medium continues to move backwards while the output vacuum peak moves to the right. As we mentioned earlier, such

output peaks that have exited before the input peaks have entered the gain medium, including the backward moving peaks, have been observed experimentally [298].

A MATLAB movie of this example may be seen by running the file `grvmovie1.m` in the `movies` subdirectory of the ewa toolbox. See also the movie `grvmovie2.m` in which the carrier frequency has been increased and corresponds to a superluminal group velocity ($v_g > c$) for the gain medium. In this case, which is also described in Problem 3.10, all the peaks are moving forward.

3.10 Chirp Radar and Pulse Compression

Pulse Radar Requirements

The chirping and dispersion compensation concepts discussed in the previous sections are applicable also to chirp radar systems. Here, we give a brief introduction to the main ideas [343] and the need for pulse compression.

In radar, the propagation medium is assumed to be non-dispersive (e.g., air), hence, it introduces only a propagation delay. Chirping is used to increase the bandwidth of the transmitted radar pulses, while keeping their time-duration long. The received pulses are processed by a dispersion compensation filter that cancels the frequency dispersion introduced by chirping and results in a time-compressed pulse. The basic system is shown in Fig. 3.10.1. The technique effectively combines the benefits of a long-duration pulse (improved detectability and Doppler resolution) with those of a broadband pulse (improved range resolution.)

A typical pulsed radar sends out sinusoidal pulses of some finite duration of, say, T seconds. A pulse reflected from a stationary target at a distance R returns back at the radar attenuated and with an overall round-trip delay of $t_d = 2R/c$ seconds. The range R is determined from the delay t_d. An uncertainty in measuring t_d from two nearby targets translates into an uncertainty in the range, $\Delta R = c(\Delta t_d)/2$. Because the pulse has duration T, the uncertainty in t_d will be $\Delta t_d = T$, and the uncertainty in the range, $\Delta R = cT/2$. Thus, to improve the range resolution, a short pulse duration T must be used.
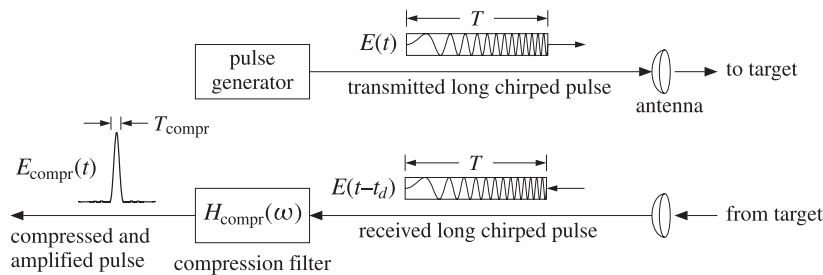

Fig. 3.10.1 Chirp radar system.

On the other hand, the detectability of the received pulse requires a certain minimum value of the signal-to-noise ratio (SNR), which in turn, requires a large value of T. The SNR at the receiver is given by

$$\text{SNR} = \frac{\mathcal{E}_{\text{rec}}}{N_0} = \frac{P_{\text{rec}}T}{N_0}$$

where P_{rec} and $\mathcal{E}_{\text{rec}} = P_{\text{rec}}T$ denote the power and energy of the received pulse, and N_0 is the noise power spectral density given in terms of the effective noise temperature T_e of the receiver by $N_0 = kT_e$ (as discussed in greater detail in Sec. 15.7). It follows from the radar equation (15.11.4) of Sec. 15.11, that the received power P_{rec} is proportional to the transmitter power P_{tr} and inversely proportional to the fourth power of the distance R. Thus, to keep the SNR at detectable levels for large distances, a large transmitter power and corresponding pulse energy $\mathcal{E}_{\text{tr}} = P_{\text{tr}}T$ must be used. This can be achieved by increasing T, while keeping P_{tr} at manageable levels.

The Doppler velocity resolution, similarly, improves with increasing T. The Doppler frequency shift for a target moving at a radial velocity v is $f_d = 2f_0v/c$, where f_0 is the carrier frequency. We will see below that the uncertainty in f_d is given roughly by $\Delta f_d = 1/T$. Thus, the uncertainty in speed will be $\Delta v = c(\Delta f_d)/2f_0 = c/(2f_0T)$.

The simultaneous conflicting requirements of a short duration T to improve the resolution in range, and a large duration T to improve the detectability of distant targets and Doppler resolution, can be realized by sending out a pulse that has both a long duration T and a very large bandwidth of, say, B Hertz, such that $BT \gg 1$. Upon reception, the received pulse can be compressed with the help of a compression filter to the much shorter duration of $T_{\text{compr}} = 1/B$ seconds, which satisfies $T_{\text{compr}} = 1/B \ll T$. The improvement in range resolution will be then $\Delta R = cT_{\text{compr}}/2 = c/2B$.

In summary, the following formulas capture the tradeoffs among the three requirements of detectability, range resolution, and Doppler resolution:

$$\text{SNR} = \frac{\mathcal{E}_{\text{rec}}}{N_0} = \frac{P_{\text{rec}}T}{N_0}, \quad \Delta R = \frac{c}{2B}, \quad \Delta v = \frac{c}{2f_0T} \tag{3.10.1}$$

For example, to achieve a 30-meter range resolution and a 50 m/s (180 km/hr) velocity resolution at a 3-GHz carrier frequency, would require $B = 5$ MHz and $T = 1$ msec, resulting in the large time-bandwidth product of $BT = 5000$.

Such large time-bandwidth products cannot be achieved with plain sinusoidal pulses. For example, an ordinary, unchirped, sinusoidal rectangular pulse of duration of T seconds has an effective bandwidth of $B = 1/T$ Hertz, and hence, $BT = 1$. This follows from the Fourier transform pair:

$$E(t) = \text{rect}\left(\frac{t}{T}\right)e^{j\omega_0 t} \quad \Leftrightarrow \quad \hat{E}(\omega) = T\frac{\sin((\omega - \omega_0)T/2)}{(\omega - \omega_0)T/2} \tag{3.10.2}$$

where $\text{rect}(x)$ is the rectangular pulse defined with the help of the unit step $u(x)$:

$$\text{rect}(x) = u(x + 0.5) - u(x - 0.5) = \begin{cases} 1, & \text{if } |x| < 0.5 \\ 0, & \text{if } |x| > 0.5 \end{cases}$$

It follows from (3.10.2) that the 3-dB width of the spectrum is $\Delta\omega = 0.886(2\pi)/T$, or in Hz, $\Delta f = 0.886/T$, and similarly, the quantity $\Delta f = 1/T$ represents the 4-dB width. Thus, the effective bandwidth of the rectangular pulse is $1/T$.

Linear FM Signals

It is possible, nevertheless, to have a waveform whose envelope has an arbitrary duration T while its spectrum has an arbitrary width B, at least in an approximate sense. The key idea in accomplishing this is to have the *instantaneous frequency* of the signal vary—during the duration T of the envelope—over a set of values that *span* the desired bandwidth B. Such time variation of the instantaneous frequency translates in the frequency domain to a spectrum of effective width B.

The simplest realization of this idea is through *linear FM*, or chirping, that corresponds to a linearly varying instantaneous frequency. More complicated schemes exist that use nonlinear time variations, or, using phase-coding in which the instantaneous phase of the signal changes by specified amounts during the duration T in such a way as to broaden the spectrum. A chirped pulse is given by:

$$E(t) = F(t)\,e^{j\omega_0 t + j\dot{\omega}_0 t^2/2} \qquad (3.10.3)$$

where $F(t)$ is an arbitrary envelope with an effective duration T, defined for example over the time interval $-T/2 \le t \le T/2$. The envelope $F(t)$ can be specified either in the time domain or in the frequency domain by means of its spectrum $\hat{F}(\omega)$:

$$\hat{F}(\omega) = \int_{-\infty}^{\infty} F(t)\,e^{-j\omega t}\,dt \quad \Leftrightarrow \quad F(t) = \frac{1}{2\pi}\int_{-\infty}^{\infty} \hat{F}(\omega)\,e^{j\omega t}\,d\omega \qquad (3.10.4)$$

Typically, $F(t)$ is real-valued and therefore, the instantaneous frequency of (3.10.3) is $\omega(t) = \dot{\theta}(t) = \omega_0 + \dot{\omega}_0 t$. During the time interval $-T/2 \le t \le T/2$, it varies over the band $\omega_0 - \dot{\omega}_0 T/2 \le \omega(t) \le \omega_0 + \dot{\omega}_0 T/2$, (we are assuming here that $\dot{\omega}_0 > 0$.) Hence, it has an effective total bandwidth:

$$\Omega = \dot{\omega}_0 T, \quad \text{or, in units of Hz}, \quad B = \frac{\Omega}{2\pi} = \frac{\dot{\omega}_0 T}{2\pi} \qquad (3.10.5)$$

Thus, given T and B, the chirping parameter can be chosen to be $\dot{\omega}_0 = 2\pi B/T$. We will look at some examples of $F(t)$ shortly and confirm that the spectrum of the chirped signal $E(t)$ is effectively confined in the band $|f - f_0| \le B/2$. But first, we determine the compression filter.

Pulse Compression Filter

The received signal reflected from a target is an attenuated and delayed copy of the transmitted signal $E(t)$, that is,

$$E_{\text{rec}}(t) = a E(t - t_d) = a F(t - t_d)\,e^{j\omega_0(t-t_d) + j\dot{\omega}_0(t-t_d)^2/2} \qquad (3.10.6)$$

where a is an attenuation factor determined from the radar equation to be the ratio of the received to the transmitted powers: $a^2 = P_{\text{rec}}/P_{\text{tr}}$.

If the target is moving with a radial velocity v towards the radar, there will be a Doppler shift by $\omega_d = 2v\omega_0/c$. Although this shift affects all the frequency components, that is, $\omega \to \omega + \omega_d$, it is common to make the so-called narrowband approximation in which only the carrier frequency is shifted $\omega_0 \to \omega_0 + \omega_d$. This is justified

for radar signals because, even though the bandwidth Ω is wide, it is still only a small fraction (typically one percent) of the carrier frequency, that is, $\Omega \ll \omega_0$. Thus, the received signal from a moving target is taken to be:

$$E_{\text{rec}}(t) = a E(t - t_d)\,e^{j\omega_d(t-t_d)} = a F(t - t_d)\,e^{j(\omega_0+\omega_d)(t-t_d) + j\dot{\omega}_0(t-t_d)^2/2} \qquad (3.10.7)$$

To simplify the notation, we will ignore the attenuation factor and the delay, which can be restored at will later, and take the received signal to be:

$$\boxed{E_{\text{rec}}(t) = E(t)\,e^{j\omega_d t} = F(t)\,e^{j(\omega_0+\omega_d)t + j\dot{\omega}_0 t^2/2}} \qquad (3.10.8)$$

This signal is then processed by a pulse compression filter that will compress the waveform to a shorter duration. To determine the specifications of the compression filter, we consider the unrealizable case of a signal that has infinite duration and infinite bandwidth defined by $F(t) = 1$, for $-\infty < t < \infty$. For now, we will ignore the Doppler shift so that $E_{\text{rec}}(t) = E(t)$. Using Eq. (3.5.18), the chirped signal and its spectrum are:

$$E(t) = e^{j\omega_0 t + j\dot{\omega}_0 t^2/2} \quad \Leftrightarrow \quad \hat{E}(\omega) = \sqrt{\frac{2\pi j}{\dot{\omega}_0}}\,e^{-j(\omega-\omega_0)^2/2\dot{\omega}_0} \qquad (3.10.9)$$

Clearly, the magnitude spectrum is constant and has infinite extent spanning the entire frequency axis. The compression filter must equalize the quadratic phase spectrum of the signal, that is, it must have the opposite phase:

$$\boxed{H_{\text{compr}}(\omega) = e^{j(\omega-\omega_0)^2/2\dot{\omega}_0}} \quad \text{(pulse compression filter)} \qquad (3.10.10)$$

The corresponding impulse response is the inverse Fourier transform of Eq. (3.10.10):

$$\boxed{h_{\text{compr}}(t) = \sqrt{\frac{j\dot{\omega}_0}{2\pi}}\,e^{j\omega_0 t - j\dot{\omega}_0 t^2/2}} \quad \text{(pulse compression filter)} \qquad (3.10.11)$$

The resulting output spectrum for the input (3.10.9) will be:

$$\hat{E}_{\text{compr}}(\omega) = H_{\text{compr}}(\omega)\,\hat{E}(\omega) = \sqrt{\frac{2\pi j}{\dot{\omega}_0}}\,e^{-j(\omega-\omega_0)^2/2\dot{\omega}_0} \cdot e^{j(\omega-\omega_0)^2/2\dot{\omega}_0} = \sqrt{\frac{2\pi j}{\dot{\omega}_0}}$$

that is, a constant for all ω. Hence, the input signal gets compressed into a Dirac delta:

$$E_{\text{compr}}(t) = \sqrt{\frac{2\pi j}{\dot{\omega}_0}}\,\delta(t) \qquad (3.10.12)$$

When the envelope $F(t)$ is a finite-duration signal, the resulting spectrum of the chirped signal $E(t)$ still retains the essential quadratic phase of Eq. (3.10.9), and therefore, the compression filter will still be given by Eq. (3.10.10) for all choices of $F(t)$. Using the stationary-phase approximation, Problem 3.17 shows that the quadratic phase is a general property. The group delay of this filter is given by Eq. (3.2.1):

$$t_g = -\frac{d}{d\omega}\left[\frac{(\omega-\omega_0)^2}{2\dot{\omega}_0} \right] = -\frac{\omega-\omega_0}{\dot{\omega}_0} = -\frac{2\pi(f-f_0)}{2\pi B/T} = -T\frac{f-f_0}{B}$$

As the frequency $(f - f_0)$ increases from $-B/2$ to $B/2$, the group delay *decreases* from $T/2$ to $-T/2$, that is, the lower frequency components, which occur earlier in the chirped pulse, suffer a longer delay through the filter. Similarly, the high frequency components, which occur later in the pulse, suffer a shorter delay, the overall effect being the time compression of the pulse.

It is useful to demodulate the sinusoidal carrier $e^{j\omega_0 t}$ and write $h_{\text{compr}}(t) = e^{j\omega_0 t} g(t)$ and $H_{\text{compr}}(\omega) = G(\omega - \omega_0)$, where the demodulated "baseband" filter, which is known as a *quadrature-phase filter*, is defined by:

$$\boxed{g(t) = \sqrt{\frac{j\dot{\omega}_0}{2\pi}}\, e^{-j\dot{\omega}_0 t^2/2}, \quad G(\omega) = e^{j\omega^2/2\dot{\omega}_0}} \quad \text{(quadratic phase filter)} \qquad (3.10.13)$$

For an arbitrary envelope $F(t)$, one can derive the following fundamental result that relates the *output* of the compression filter (3.10.11) to the *Fourier transform*, $\hat{F}(\omega)$, of the envelope, when the input is $E(t) = F(t) e^{j\omega_0 t + j\dot{\omega}_0 t^2/2}$:

$$\boxed{E_{\text{compr}}(t) = \sqrt{\frac{j\dot{\omega}_0}{2\pi}}\, e^{j\omega_0 t - j\dot{\omega}_0 t^2/2}\, \hat{F}(-\dot{\omega}_0 t)} \qquad (3.10.14)$$

This result belongs to a family of so-called "chirp transforms" or "Fresnel transforms" that find application in optics, the diffraction effects of lenses [1186], and in other areas of signal processing, such as for example, the "chirp z-transform" [48]. To show Eq. (3.10.14), we use the convolutional definition for the filter output:

$$E_{\text{compr}}(t) = \int_{-\infty}^{\infty} h_{\text{compr}}(t - t')\, E(t')\, dt'$$

$$= \sqrt{\frac{j\dot{\omega}_0}{2\pi}} \int_{-\infty}^{\infty} e^{j\omega_0(t-t') - j\dot{\omega}_0(t-t')^2/2}\, F(t')\, e^{j\omega_0 t' + j\dot{\omega}_0 t'^2/2}\, dt'$$

$$= \sqrt{\frac{j\dot{\omega}_0}{2\pi}}\, e^{j\omega_0 t - j\dot{\omega}_0 t^2/2} \int_{-\infty}^{\infty} F(t')\, e^{j(\dot{\omega}_0 t)t'}\, dt'$$

where the last integral factor is recognized as $\hat{F}(-\dot{\omega}_0 t)$. As an example, Eq. (3.10.12) can be derived immediately by noting that $F(t) = 1$ has the Fourier transform $\hat{F}(\omega) = 2\pi\delta(\omega)$, and therefore, using Eq. (3.10.14), we have:

$$E_{\text{compr}}(t) = \sqrt{\frac{j\dot{\omega}_0}{2\pi}}\, e^{j\omega_0 t - j\dot{\omega}_0 t^2/2}\, 2\pi\delta(-\dot{\omega}_0 t) = \sqrt{\frac{2\pi j}{\dot{\omega}_0}}\, \delta(t)$$

where we used the property $\delta(-\dot{\omega}_0 t) = \delta(\dot{\omega}_0 t) = \delta(t)/\dot{\omega}_0$ and set $t = 0$ in the exponentials.

The property (3.10.14) is shown pictorially in Fig. 3.10.2. This arrangement can also be thought of as a real-time spectrum analyzer of the input envelope $F(t)$.

In order to remove the chirping factor $e^{-j\dot{\omega}_0 t^2/2}$, one can prefilter $F(t)$ with the baseband filter $G(\omega)$ and then apply the above result to its output. This leads to a modified compressed output given by:

$$\bar{E}_{\text{compr}}(t) = \sqrt{\frac{j\dot{\omega}_0}{2\pi}}\, e^{j\omega_0 t}\, \hat{F}(-\dot{\omega}_0 t) \qquad (3.10.15)$$
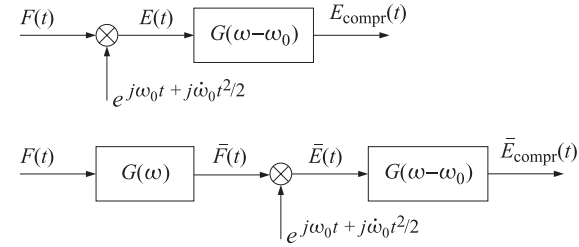
Fig. 3.10.2 Pulse compression filter.

Fig. 3.10.2 also depicts this property. To show it, we note the identity:

$$e^{j\omega_0 t - j\dot{\omega}_0 t^2/2}\, \hat{F}(-\dot{\omega}_0 t) = e^{j\omega_0 t} \left[e^{-j\omega^2/2\dot{\omega}_0}\, \hat{F}(\omega) \right]_{\omega = -\dot{\omega}_0 t}$$

Thus, if in this expression $\hat{F}(\omega)$ is replaced by its prefiltered version $G(\omega)\hat{F}(\omega)$, then the quadratic phase factor will be canceled leaving only $\hat{F}(\omega)$.

For a moving target, the envelope $F(t)$ is replaced by $F(t) e^{j\omega_d t}$, and $\hat{F}(\omega)$ is replaced by $\hat{F}(\omega - \omega_d)$, and similarly, $\hat{F}(-\dot{\omega}_0 t)$ is replaced by $\hat{F}(-\dot{\omega}_0 t - \omega_d)$. Thus, Eq. (3.10.14) is modified as follows:

$$\boxed{E_{\text{compr}}(t) = \sqrt{\frac{j\dot{\omega}_0}{2\pi}}\, e^{j\omega_0 t - j\dot{\omega}_0 t^2/2}\, \hat{F}\big(-(\omega_d + \dot{\omega}_0 t)\big)} \qquad (3.10.16)$$

Chirped Rectangular Pulse

Next, we discuss the practical case of a rectangular envelope of duration T:

$$F(t) = \text{rect}\left(\frac{t}{T}\right) \quad \Rightarrow \quad E(t) = \text{rect}\left(\frac{t}{T}\right) e^{j\omega_0 t + j\dot{\omega}_0 t^2/2} \qquad (3.10.17)$$

From Eq. (3.10.2), the Fourier transform of $F(t)$ is,

$$\hat{F}(\omega) = T\frac{\sin(\omega T/2)}{\omega T/2}$$

Therefore, the output of the compression filter will be:

$$E_{\text{compr}}(t) = \sqrt{\frac{j\dot{\omega}_0}{2\pi}}\, e^{j\omega_0 t - j\dot{\omega}_0 t^2/2}\, \hat{F}(-\dot{\omega}_0 t) = \sqrt{\frac{j\dot{\omega}_0}{2\pi}}\, e^{j\omega_0 t - j\dot{\omega}_0 t^2/2}\, T\frac{\sin(-\dot{\omega}_0 tT/2)}{-\dot{\omega}_0 tT/2}$$

Noting that $\dot{\omega}_0 T = \Omega = 2\pi B$ and that $\sqrt{j\dot{\omega}_0 T^2/2\pi} = \sqrt{jBT}$, we obtain:

$$\boxed{E_{\text{compr}}(t) = \sqrt{jBT}\, e^{j\omega_0 t - j\dot{\omega}_0 t^2/2}\, \frac{\sin(\pi Bt)}{\pi Bt}} \qquad (3.10.18)$$

The sinc-function envelope $\sin(\pi Bt)/\pi Bt$ has an effective compressed width of $T_{\text{compr}} = 1/B$ measured at the 4-dB level. Moreover, the height of the peak is boosted by a factor of $\sqrt{BT}$.

Fig. 3.10.3 shows a numerical example with the parameter values $T = 30$ and $B = 4$ (in arbitrary units), and $\omega_0 = 0$. The left graph plots the real part of $E(t)$ of Eq. (3.10.17). The right graph is the real part of Eq. (3.10.18), where because of the factor $\sqrt{j}$, the peak reaches the maximum value of $\sqrt{BT}/\sqrt{2}$.
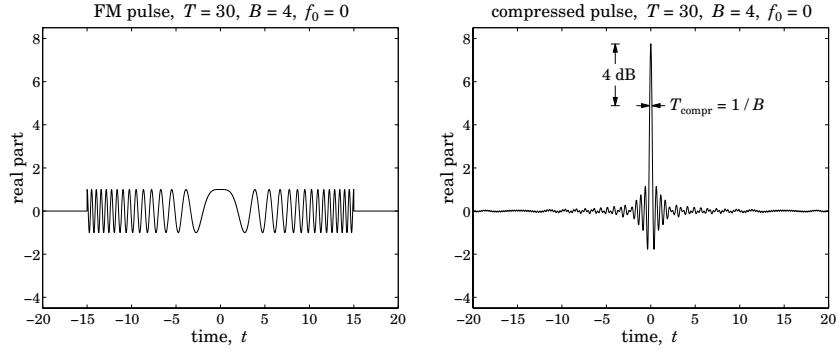

Fig. 3.10.3　FM pulse and its compressed version, with $T = 30$, $B = 4$, $f_0 = 0$.

We may also determine the Fourier transform of $E(t)$ of Eq. (3.10.17) and verify that it is primarily confined in the band $|f - f_0| \leq B/2$. We have:

$$\hat{E}(\omega) = \int_{-\infty}^{\infty} E(t) e^{-j\omega t}\, dt = \int_{-T/2}^{T/2} e^{j\omega_0 t + j\dot{\omega}_0 t^2/2} e^{-j\omega t}\, dt$$

After changing variables from t to $u = \sqrt{\dot{\omega}_0/\pi}\,[t - (\omega - \omega_0)/\dot{\omega}_0]$, this integral can be reduced to the complex Fresnel integral $\mathcal{F}(x) = C(x) - jS(x) = \int_0^x e^{-j\pi u^2/2}\, du$ discussed in greater detail in Appendix F. The resulting spectrum then takes the form:

$$\hat{E}(\omega) = \sqrt{\frac{\pi}{\dot{\omega}_0}}\, e^{-j(\omega-\omega_0)^2/2\dot{\omega}_0}\, [\mathcal{F}(w_+) - \mathcal{F}(w_-)]^*$$

which can be written in the normalized form:

$$\hat{E}(\omega) = \sqrt{\frac{2\pi j}{\dot{\omega}_0}}\, e^{-j(\omega-\omega_0)^2/2\dot{\omega}_0}\, D^*(\omega)\,, \quad D(\omega) = \frac{\mathcal{F}(w_+) - \mathcal{F}(w_-)}{1 - j} \qquad (3.10.19)$$

where $w_\pm$ are defined by:

$$w_\pm = \sqrt{\frac{\dot{\omega}_0}{\pi}}\left(\pm\frac{T}{2} - \frac{\omega - \omega_0}{\dot{\omega}_0}\right) = \sqrt{2BT}\left(\pm\frac{1}{2} - \frac{f - f_0}{B}\right) \qquad (3.10.20)$$

Eq. (3.10.19) has the expected quadratic phase term and differs from (3.10.9) by the factor $D^*(\omega)$. This factor has a magnitude that is effectively confined within the ideal band $|f - f_0| \leq B/2$ and a phase that remains almost zero within the same band, with both of these properties improving with increasing time-bandwidth product BT.[†] Thus,

---

[†] The denominator $(1 - j)$ in $D(\omega)$ is due to the asymptotic value of $\mathcal{F}(\infty) = (1 - j)/2$.

the choice for the compression filter that was made on the basis of the quadratic phase term is justified.

Fig. 3.10.4 displays the spectrum $\hat{E}(\omega)$ for the values $T = 30$ and $B = 4$, and $\omega_0 = 0$. The left and right graphs plot the magnitude and phase of the quantity $D^*(\omega)$. For comparison, the spectrum of an ordinary, unchirped, pulse of the same duration $T = 30$, given by Eq. (3.10.2), is also shown on the magnitude graph. The Fresnel functions were evaluated with the help of the MATLAB function `fcs.m` of Appendix F. The ripples that appear in the magnitude and phase are due to the Fresnel functions.
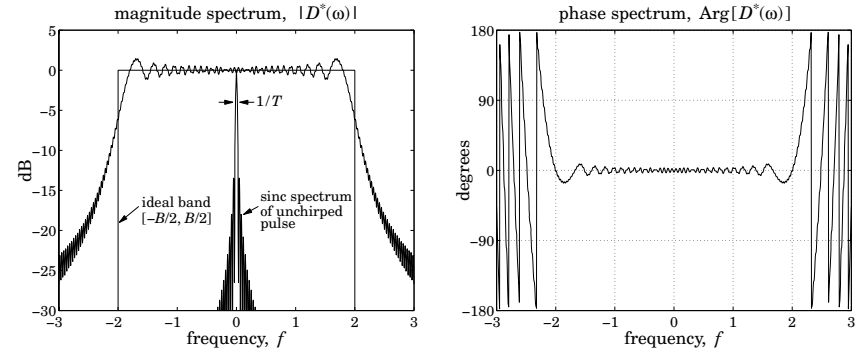

Fig. 3.10.4　Frequency spectrum of FM pulse, with $T = 30$, $B = 4$, $f_0 = 0$.

Doppler Ambiguity

For a moving target causing a Doppler shift ω_d, the output will be given by Eq. (3.10.16), which for the rectangular pulse gives:

$$E_{\mathrm{compr}}(t) = \sqrt{\frac{j\dot{\omega}_0}{2\pi}}\, e^{j\omega_0 t - j\dot{\omega}_0 t^2/2}\, T\, \frac{\sin((\omega_d + \dot{\omega}_0 t)T/2)}{(\omega_d + \dot{\omega}_0 t)T/2}$$

Noting that $(\omega_d + \dot{\omega}_0 t)T = 2\pi(f_d T + Bt)$, and replacing t by $t - t_d$ to restore the actual delay of arrival of the received pulse, we obtain:

$$E_{\mathrm{compr}}(t, f_d) = \sqrt{jBT}\, e^{j\omega_0(t-t_d) - j\dot{\omega}_0(t-t_d)^2/2}\, \frac{\sin[\pi(f_d T + B(t - t_d))]}{\pi(f_d T + B(t - t_d))} \qquad (3.10.21)$$

It is seen that the peak of the pulse no longer takes place at $t = t_d$, but rather at the shifted time $f_d T + B(t - t_d) = 0$, or, $t = t_d - f_d T/B$, resulting in a potential ambiguity in the range. Eq. (3.10.21) is an example of an *ambiguity function* commonly used in radar to quantify the simultaneous uncertainty in range and Doppler. Setting $t = t_d$, we find:

$$E_{\mathrm{compr}}(t_d, f_d) = \sqrt{jBT}\, \frac{\sin(\pi f_d T)}{\pi f_d T} \qquad (3.10.22)$$

which shows that the Doppler resolution is $\Delta f_d = 1/T$, as we discussed at the beginning.

Sidelobe Reduction

Although the filter output (3.10.18) is highly compressed, it has significant sidelobes that are approximately 13 dB down from the main lobe. Such sidelobes, referred to as "range sidelobes," can mask the presence of small nearby targets.

The sidelobes can be suppressed using windowing, which can be applied either in the time domain or the frequency domain. To reduce sidelobes in one domain (frequency or time), one must apply windowing to the conjugate domain (time or frequency).

Because the compressed output envelope is the Fourier transform $\hat{F}(\omega)$ evaluated at $\omega = -\dot{\omega}_0 t$, the sidelobes can be suppressed by applying a time window $w(t)$ of length T to the envelope, that is, replacing $F(t)$ by $F_w(t) = w(t)F(t)$. Alternatively, to reduce the sidelobes in the time signal $\hat{F}(-\dot{\omega}_0 t)$, one can apply windowing to its Fourier transform, which can be determined as follows:

$$\hat{\hat{F}}(\omega) = \int_{-\infty}^{\infty} \hat{F}(-\dot{\omega}_0 t) e^{-j\omega t} dt = \int_{-\infty}^{\infty} \hat{F}(\omega') e^{j\omega\omega'/\dot{\omega}_0} d\omega'/\dot{\omega}_0 = \frac{2\pi}{\dot{\omega}_0} F(\omega/\dot{\omega}_0)$$

that is, the time-domain envelope $F(t)$ evaluated at $t = \omega/\dot{\omega}_0$. Thus, a time window $w(t)$ can just as well be applied in the frequency domain in the form:

$$\hat{\hat{F}}(\omega) = F(\omega/\dot{\omega}_0) \quad \Rightarrow \quad \hat{\hat{F}}_w(\omega) = w(\omega/\dot{\omega}_0)F(\omega/\dot{\omega}_0)$$

Since $w(t)$ is concentrated over $-T/2 \le t \le T/2$, the frequency window $w(\omega/\dot{\omega}_0)$ will be concentrated over

$$-\frac{T}{2} \le \frac{\omega}{\dot{\omega}_0} \le \frac{T}{2} \quad \Rightarrow \quad -\frac{\Omega}{2} \le \omega \le \frac{\Omega}{2}$$

where $\Omega = \dot{\omega}_0 T = 2\pi B$. For example, a Hamming window, which affords a suppression of the sidelobes by 40 dB, can be applied in the time or frequency domain:

$$w(t) = 1 + 2\alpha \cos\left(\frac{2\pi t}{T}\right), \quad -\frac{T}{2} \le t \le \frac{T}{2}$$

$$w(\omega/\dot{\omega}_0) = 1 + 2\alpha \cos\left(\frac{2\pi\omega}{\Omega}\right), \quad -\frac{\Omega}{2} \le \omega \le \frac{\Omega}{2} \tag{3.10.23}$$

where $2\alpha = 0.46/0.54$, or, $\alpha = 0.4259$.[†] The time-domain window can be implemented in a straightforward fashion using delays. Writing $w(t)$ in exponential form, we have

$$w(t) = 1 + \alpha\left[e^{2\pi jt/T} + e^{-2\pi jt/T}\right]$$

The spectrum of $F_w(t) = w(t)F(t) = \left(1 + \alpha\left[e^{2\pi jt/T} + e^{-2\pi jt/T}\right]\right)F(t)$ will be:

$$\hat{F}_w(\omega) = \hat{F}(\omega) + \alpha\left[\hat{F}(\omega - 2\pi/T) + \hat{F}(\omega + 2\pi/T)\right]$$

Thus, the envelope of the compressed signal will be:

$$\hat{F}_w(-\dot{\omega}_0 t) = \hat{F}(-\dot{\omega}_0 t) + \alpha\left[\hat{F}(-\dot{\omega}_0 t - 2\pi/T) + \hat{F}(-\dot{\omega}_0 t + 2\pi/T)\right]$$

$$= \hat{F}(-\dot{\omega}_0 t) + \alpha\left[\hat{F}(-\dot{\omega}_0(t + T_{\text{compr}})) + \hat{F}(-\dot{\omega}_0(t - T_{\text{compr}}))\right]$$

[†]This definition of $w(t)$ differs from the ordinary Hamming window by a factor of 0.54.

where $T_{\text{compr}} = 2\pi T/\dot{\omega}_0 = 1/B$. It follows that the compressed output will be:

$$E_{\text{compr}}(t) = \sqrt{jBT}\, e^{j\omega_0 t - j\dot{\omega}_0 t^2/2}\, \left[\text{sinc}(Bt) + \alpha\,\text{sinc}(Bt+1) + \alpha\,\text{sinc}(Bt-1)\right] \tag{3.10.24}$$

where $\text{sinc}(x) = \sin(\pi x)/\pi x$, and we wrote $B(t \pm T_{\text{compr}}) = (Bt \pm 1)$. Fig. 3.10.5 shows the Hamming windowed chirped pulse and the corresponding compressed output computed from Eq. (3.10.24).
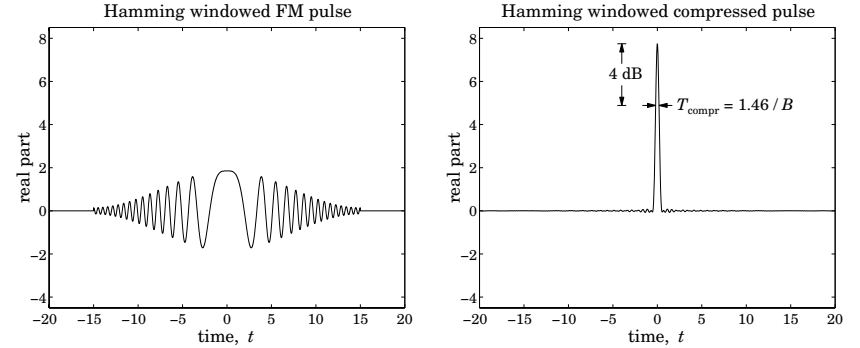

Fig. 3.10.5 Hamming windowed FM pulse and its compressed version, with $T = 30$, $B = 4$.

The price to pay for reducing the sidelobes is a somewhat wider mainlobe width. Measured at the 4-dB level, the width of the compressed pulse is $T_{\text{compr}} = 1.46/B$, as compared with $1/B$ in the unwindowed case.

Matched Filter

A more appropriate choice for the compression filter is the *matched filter*, which maximizes the receiver's SNR. Without getting into the theoretical justification, a filter matched to a transmitted waveform $E(t)$ has the conjugate-reflected impulse response $h(t) = E^*(-t)$ and corresponding frequency response $H(\omega) = \hat{E}^*(\omega)$. In particular for the rectangular chirped pulse, we have:

$$E(t) = \text{rect}\left(\frac{t}{T}\right) e^{j\omega_0 t + j\dot{\omega}_0 t^2/2} \quad \Rightarrow \quad h(t) = E^*(-t) = \text{rect}\left(\frac{t}{T}\right) e^{j\omega_0 t - j\dot{\omega}_0 t^2/2} \tag{3.10.25}$$

which differs from our simplified compression filter by the factor $\text{rect}(t/T)$. Its frequency response is given by the conjugate of Eq. (3.10.19)

$$H(\omega) = \sqrt{-\frac{2\pi j}{\dot{\omega}_0}}\, e^{j(\omega-\omega_0)^2/2\dot{\omega}_0}\, D(\omega)\,, \quad D(\omega) = \frac{\mathcal{F}(w_+) - \mathcal{F}(w_-)}{1-j} \tag{3.10.26}$$

We have seen that the factor $D(\omega)$ is essentially unity within the band $|f - f_0| \le B/2$. Thus again, the matched filter resembles the filter (3.10.10) within this band. The resulting output of the matched filter is remarkably similar to that of Eq. (3.10.18):

$$E_{\text{compr}}(t) = e^{j\omega_0 t}\, T\, \frac{\sin(\pi B|t| - \pi Bt^2/T)}{\pi B|t|}, \quad \text{for} \quad -T \le t \le T \tag{3.10.27}$$

while it vanishes for $|t| > T$.

In practice, the matched/compression filters are conveniently realized either digitally using digital signal processing (DSP) techniques or using surface acoustic wave (SAW) devices [368]. Similarly, the waveform generator of the chirped pulse may be realized using DSP or SAW methods. A convenient generation method is to send an impulse (or, a broadband pulse) to the input of a filter that has as frequency response $H(\omega) = \hat{E}(\omega)$, so that the impulse response of the filter is the signal $E(t)$ that we wish to generate.

Signal design in radar is a subject in itself and the present discussion was only meant to be an introduction motivated by the similarity to dispersion compensation.

3.11 Further Reading

The topics discussed in this chapter are vast and diverse. The few references given below are inevitably incomplete.

References [153–176] discuss the relationship between group velocity and energy velocity for lossless or lossy media, as well as the issue of electromagnetic field momentum and radiation pressure.

Some references on pulse propagation, spreading, chirping, and dispersion compensation in optical fibers, plasmas, and other media are [177–229], while precursors are discussed in Sommerfeld [1135], Brillouin [177], and [230–242].

Some theoretical and experimental references on fast and negative group velocity are [243–298]. Circuit realizations of negative group delays are discussed in [299–303]. References [304–335] discuss slow light and electromagnetically induced transparency and related experiments.

Some references on chirp radar and pulse compression are [336–375]. These include phase-coding methods, as well as alternative phase modulation methods for Doppler-resistant applications.

3.12 Problems

3.1 Using the definitions (3.2.5), show that the group and phase velocities are related by:

$$v_g = v_p + \beta \frac{dv_p}{d\beta}$$

3.2 It was mentioned earlier that when $v_g > c$, the peak of a pulse shifts forward in time as it propagates. With reference to Fig. 3.2.2, let t_{peak} be the time of the peak of the initial pulse $E(0, t)$. First, show that the peak of the propagated pulse $E(z, t)$ occurs at time $t_{\text{prop}} = t_{\text{peak}} + z/v_g$. Then, show that the peak value $E(z, t_{\text{prop}})$ does not depend on the initial peak $E(0, t_{\text{peak}})$ but rather it depends causally on the values $E(0, t)$, for $t_0 \le t \le t_{\text{peak}} - \Delta t$, where $\Delta t = z/c - z/v_g$, which is positive if $v_g > c$. What happens if $0 < v_g < c$ and if $v_g < 0$?

3.3 Consider case 6 of the exactly solvable examples of Sec. 3.3 describing a lossy transmission line with distributed parameters L', C', R', G'. The voltage and current along the line satisfy

the so-called telegrapher's equations:

$$\frac{\partial V}{\partial z} + L' \frac{\partial I}{\partial t} + R' I = 0, \qquad \frac{\partial I}{\partial z} + C' \frac{\partial V}{\partial t} + G' V = 0 \tag{3.12.1}$$

The voltage impulse response $V(z, t)$ of the line is given by Eq. (3.3.1), where $t_f = z/c$, $a + b = R'/L'$, $a - b = G'/C'$, and $c = 1/\sqrt{L'C'}$:

$$V(z, t) = \delta(t - t_f) e^{-a t_f} + e^{-at} \frac{I_1\left(b\sqrt{t^2 - t_f^2}\right)}{\sqrt{t^2 - t_f^2}} b t_f \, u(t - t_f)$$

Show that the corresponding current $I(z, t)$ is given by

$$\sqrt{\frac{L'}{C'}} I(z, t) = \delta(t - t_f) e^{-a t_f} + e^{-at} \left[\frac{I_1\left(b\sqrt{t^2 - t_f^2}\right)}{\sqrt{t^2 - t_f^2}} bt - b I_0\left(b\sqrt{t^2 - t_f^2}\right) \right] u(t - t_f)$$

by verifying that V and I satisfy Eqs. (3.12.1). *Hint:* Use the relationships: $I_0'(x) = I_1(x)$ and $I_1'(x) = I_0(x) - I_1(x)/x$ between the Bessel functions $I_0(x)$ and $I_1(x)$.

Next, show that the Fourier transforms of $V(z, t)$ and $I(z, t)$ are:

$$\hat{V}(z, \omega) = e^{-\gamma z}, \qquad \hat{I}(z, \omega) = \frac{e^{-\gamma z}}{Z}$$

where γ, Z are the propagation constant and characteristic impedance (see Sec. 10.6):

$$\gamma = jk = \sqrt{R' + j\omega L'}\sqrt{G' + j\omega C'}, \qquad Z = \sqrt{\frac{R' + j\omega L'}{G' + j\omega C'}}$$

3.4 *Computer Experiment—Transient Behavior.* Reproduce the results and graphs of the Figures 3.4.1, 3.4.2, and 3.4.3.

3.5 Consider the propagated envelope of a pulse under the linear approximation of Eq. (3.5.13), that is, $F(z, t) = F(0, t - k_0'z)$, for the case of a complex-valued wavenumber, $k_0' = \beta_0' - j\alpha_0'$. For a gaussian envelope:

$$F(z, t) = F(0, t - k_0'z) = \exp\left[-\frac{(t - (\beta_0' - j\alpha_0')z)^2}{2\tau_0^2} \right]$$

Determine an expression for its magnitude $|F(z, t)|$. Then show that the maximum of $|F(z, t)|$ with respect to t at a given fixed z is moving with the group velocity $v_g = 1/\beta_0'$.

Alternatively, at fixed t show that the maximum with respect to z of the snapshot $|F(z, t)|$ is moving with velocity [183]:

$$v = \frac{\beta_0'}{\beta_0'^2 - \alpha_0'^2}$$

3.6 Consider the propagating wave $E(z, t) = F(z, t) e^{j\omega_0 t - jk_0 z}$. Assuming the quadratic approximation (3.5.9), show that the envelope $F(z, t)$ satisfies the partial differential equation:

$$\left(\frac{\partial}{\partial z} + k_0' \frac{\partial}{\partial t} - j \frac{k_0''}{2} \frac{\partial^2}{\partial t^2} \right) F(z, t) = 0$$

Show that the envelope impulse response $g(z, t)$ of Eq. (3.5.16) also satisfies this equation. And that so does the gaussian pulse of Eq. (3.6.4).

3.7 Let $F(z,t)$ be the narrowband envelope of a propagating pulse as in Eq. (3.5.5). Let $z(t)$ be a point on the snapshot $F(z,t)$ that corresponds to a particular constant value of the envelope, that is, $F(z(t),t) = $ constant. Show that the point $z(t)$ is moving with velocity:

$$\dot{z}(t) = -\frac{\partial_t F}{\partial_z F}$$

Under the linear approximation of Eq. (3.5.13), show that the above expression leads to the group velocity $\dot{z}(t) = 1/k_0'$.

Alteratively, use the condition $|F(z,t)|^2 = $ constant, and show that in this case

$$\dot{z}(t) = -\frac{\mathrm{Re}(\partial_t F/F)}{\mathrm{Re}(\partial_z F/F)}$$

Under the linear approximation and assuming that the initial envelope $F(0,t)$ is real-valued, show that $\dot{z} = 1/\mathrm{Re}(k_0')$.

3.8 Given the narrowband envelope $F(z,t)$ of a propagating pulse as in Eq. (3.5.5), show that it satisfies the identity:

$$e^{-j(k-k_0)z}\hat{F}(0,\omega-\omega_0) = \int_{-\infty}^{\infty} F(z,t)\,e^{-j(\omega-\omega_0)t}\,dt$$

Define the "centroid" time $t(z)$ by the equation

$$t(z) = \frac{\int_{-\infty}^{\infty} t\,F(z,t)\,dt}{\int_{-\infty}^{\infty} F(z,t)\,dt}$$

Using the above identity, show that $t(z)$ satisfies the equation:

$$t(z) = t(0) + k_0' z \qquad (3.12.2)$$

Therefore, $t(z)$ may be thought of as a sort of group delay. Note that no approximations are needed to obtain Eq. (3.12.2).

3.9 Consider the narrowband envelope $F(z,t)$ of a propagating pulse $E(z,t) = F(z,t)e^{j\omega_0 t - jk_0 z}$ and assume that the medium is lossless so that $k(\omega)$ is real-valued. Show the identity

$$\int_{-\infty}^{\infty} |E(z,t)|^2 e^{-j\omega t}\,dt = \frac{1}{2\pi}\int_{-\infty}^{\infty} e^{jk(\omega')z}\hat{E}^*(0,\omega')\,e^{-jk(\omega'+\omega)z}\hat{E}(0,\omega'+\omega)\,d\omega'$$

Define the average time delay and average inverse group velocity through:

$$\bar{t}(z) = \frac{\int_{-\infty}^{\infty} t\,|F(z,t)|^2\,dt}{\int_{-\infty}^{\infty} |F(z,t)|^2\,dt}\,, \qquad \bar{k}_0' = \frac{\int_{-\infty}^{\infty} k'(\omega_0+\omega)|\hat{F}(0,\omega)|^2\,d\omega}{\int_{-\infty}^{\infty} |\hat{F}(0,\omega)|^2\,d\omega}$$

where $\hat{F}(0,\omega)$ is defined in Eq. (3.5.2). Using the above identity, show the relationship:

$$\bar{t}(z) = \bar{t}(0) + \bar{k}_0' z$$

3.10 *Computer Experiment—Propagation with Negative Group Velocity.* Consider the pulse propagation experiment described in Figs. 3.9.3 and 3.9.4, which is a variation of the experiment in Ref. [257]. The wavenumbers in vacuum, in the absorption and gain media will be denoted by k_v, k_a, k_g. They can be calculated from Eqs. (3.9.1)–(3.9.6) with $f = 0, +1, -1$, respectively.

Let $E(t)$ and $\hat{E}(\omega)$ be the initially launched waveform and its Fourier transform on the vacuum side of the interface with the absorbing medium at $z = 0$. Because the refractive indices $n(\omega)$ are very nearly unity, we will ignore all the reflected waves and assume that the wave enters the successive media with unity transmission coefficient.

a. Show that the wave will be given as follows in the successive media shown in Fig. 3.9.3:

$$E(z,t) = \frac{1}{2\pi}\int_{-\infty}^{\infty}\hat{E}(\omega)\,d\omega \begin{cases} e^{j\omega t - jk_v z} & \text{if } z \le 0 \\ e^{j\omega t - jk_a z} & \text{if } 0 < z \le a \\ e^{j\omega t - jk_a a - jk_v(z-a)} & \text{if } a < z \le 3a \\ e^{j\omega t - j(k_a+2k_v)a - jk_g(z-3a)} & \text{if } 3a < z \le 4a \\ e^{j\omega t - j(k_a+2k_v+k_g)a - jk_v(z-4a)} & \text{if } 4a < z \end{cases} \qquad (3.12.3)$$

Thus, in each region, the pulse will have the following form, with appropriate definitions of the wavenumbers $q(\omega), k(\omega)$, and offset d:

$$E(z,t) = \frac{1}{2\pi}\int_{-\infty}^{\infty}\hat{E}(\omega)\,e^{j\omega t - jqa - jk(z-d)}\,d\omega \qquad (3.12.4)$$

b. Consider, next, a gaussian pulse with width τ_0, modulating a carrier ω_0, defined at $z = 0$ as follows:

$$E(t) = e^{-t^2/2\tau_0^2}e^{j\omega_0 t} \quad \Leftrightarrow \quad \hat{E}(\omega) = \sqrt{2\pi\tau_0^2}\,e^{-\tau_0^2(\omega-\omega_0)^2/2} \qquad (3.12.5)$$

Assuming a sufficiently narrow bandwidth (small $1/\tau_0$ or large τ_0,) the wavenumbers $q(\omega)$ and $k(\omega)$ in Eq. (3.12.4) can be expanded up to second order about the carrier frequency ω_0 giving:

$$q(\omega) = q_0 + q_0'(\omega-\omega_0) + q_0''(\omega-\omega_0)^2/2$$
$$k(\omega) = k_0 + k_0'(\omega-\omega_0) + k_0''(\omega-\omega_0)^2/2 \qquad (3.12.6)$$

where the quantities $q_0 = q(\omega_0), q_0' = q'(\omega_0)$, etc., can be calculated from Eqs. (3.9.1)–(3.9.6). Inserting these expansions into Eq. (3.12.4), show that the pulse waveform is given by:

$$E(z,t) = e^{j\omega_0 t - jq_0 a - jk_0(z-d)}\sqrt{\frac{\tau_0^2}{\tau_0^2 + jq_0''a + jk_0''(z-d)}}$$
$$\cdot \exp\left[-\frac{(t - q_0'a - k_0'(z-d))^2}{2(\tau_0^2 + jq_0''a + jk_0''(z-d))}\right] \qquad (3.12.7)$$

c. Assume the following values of the various parameters:

$$c = 1, \quad \omega_p = 1, \quad \gamma = 0.01, \quad \omega_r = 5, \quad \tau_0 = 40, \quad a = 50, \quad \omega_0 = 5.35$$

The carrier frequency ω_0 is chosen to lie in the right wing of the resonance and lies in the negative-group-velocity range for the gain medium (this range is approximately [5.005, 5.5005] in the above frequency units.)

Calculate the values of the parameters $q_0, q_0', q_0'', k_0, k_0', k_0''$ within the various ranges of z as defined by Eq. (3.12.3), and present these values in a table form.

Thus, $E(z,t)$ can be evaluated for each value of t and for all the z's in the four ranges. Eq. (3.12.7) can easily be vectorized for each scalar t and a vector of z's.

Make a MATLAB movie of the pulse envelope $|E(z,t)|$, that is, for each successive t, plot the envelope versus z. Take z to vary over $-2a \le z \le 6a$ and t over $-100 \le t \le 300$. Such a movie can be made with the following code fragment:

```
z = -2*a : 6*a;     % vector of z's
t = -100 : 300;     % vector of t's

for i=1:length(t),

  % here insert code that calculates the vector E = E(z, t(i))

  plot(z/a, abs(E));                          % plot as function of z
  xlim([-2,6]); xtick([0,1,3,4]); grid        % keep axes the same
  ylim([0,1]); ytick(0:1:1);                  % xtick, ytick are part of ewa
  text(-1.8, 0.35, strcat('t=',num2str(t(i))), 'fontsize', 15);

  F(:,i) = getframe;       % save current frame

end

movie(F);    % replay movie - check syntax of movie() for playing options
```

Discuss your observations, and explain what happens within the absorption and gain media. An example of such a movie may be seen by running the file grvmovie1.m in the movies subdirectory of the ewa toolbox.

d. Reproduce the graphs of Fig. 3.9.4 by evaluating the snapshots at the time instants:

$$t = [-50, 0, 40, 120, 180, 220, 230, 240, 250, 260]$$

e. For both the absorbing and the gain media, plot the real and imaginary parts of the refractive index $n = n_r - jn_i$ and the real part of the group index n_g versus frequency in the interval $4 \le \omega \le 6$. Indicate on the graph the operating frequency points. For the gain case, indicate the ranges over which $\mathrm{Re}(n_g)$ is negative.

f. Repeat Parts c–d for the carrier frequency $\omega_0 = 5.8$ which lies in the superluminal range $0 < \mathrm{Re}(n_g) < 1$.

3.11 Consider Eqs. (3.9.1)–(3.9.6) for the single-resonance Lorentz model that was used in the previous experiment. Following [257], define the detuning parameters:

$$\xi = \frac{\omega - \omega_r}{\omega_p}, \quad \xi_0 = \frac{\omega_0 - \omega_r}{\omega_p} \tag{3.12.8}$$

and make the following assumptions regarding the range of these quantities:

$$\gamma \ll \omega_p \ll \omega_r \quad \text{and} \quad \frac{\omega_p}{\omega_r} \ll |\xi| \ll \frac{\omega_r}{\omega_p} \tag{3.12.9}$$

Thus, $\gamma/\omega_p \ll 1$, $\omega_p/\omega_r \ll 1$, and ξ, ξ_0 can be taken to be order of 1. In the above experiment, they were $\xi_0 = 0.35$ and $\xi_0 = 0.8$.

Show that the wavenumber $k(\omega)$, and its first and second derivatives $k'(\omega)$, $k''(\omega)$, can be expressed approximately to first order in the quantities γ/ω_p and ω_p/ω_r as follows [257]:

$$k(\omega) = \frac{\omega}{c}\left[1 - \frac{f}{4\xi}\frac{\omega_p}{\omega_r} - j\frac{f}{8\xi^2}\left(\frac{\omega_p}{\omega_r}\right)\left(\frac{\gamma}{\omega_p}\right)\right]$$

$$k'(\omega) = \frac{1}{c}\left[1 + \frac{f}{4\xi^2} + j\frac{f}{4\xi^3}\left(\frac{\gamma}{\omega_p}\right)\right]$$

$$k''(\omega) = -\frac{1}{c\omega_p}\left[\frac{f}{2\xi^3} + j\frac{3f}{4\xi^4}\left(\frac{\gamma}{\omega_p}\right)\right]$$

The group velocity v_g is obtained from the real part of $k'(\omega)$:

$$\frac{1}{v_g} = \mathrm{Re}[k'(\omega)] = \frac{1}{c}\left[1 + \frac{f}{4\xi^2}\right] \quad \Rightarrow \quad v_g = \frac{c}{1 + \dfrac{f}{4\xi^2}}$$

Thus, $v_g = c$ in vacuum ($f = 0$) and $v_g < c$ in the absorbing medium ($f = 1$). For the gain medium ($f = -1$), we have $v_g < 0$ if $|\xi| < 1/2$, and $v_g > c$ if $|\xi| > 1/2$.

Verify that this approximation is adequate for the numerical values given in the previous problem.

3.12 Consider a chirped pulse whose spectrum has an ideal rectangular shape and an ideal quadratic phase, where $\Omega = 2\pi B$ and $\dot{\omega}_0 = 2\pi B/T$:

$$\hat{E}(\omega) = \sqrt{\frac{2\pi j}{\dot{\omega}_0}}\,\mathrm{rect}\left(\frac{\omega - \omega_0}{\Omega}\right) e^{-j(\omega-\omega_0)^2/2\dot{\omega}_0}$$

This is the ideal spectrum that all waveforms in chirp radar strive to have. Show that the corresponding time signal $E(t)$ is given in terms of the Fresnel function $\mathcal{F}(x)$ by

$$E(t) = F(t)\, e^{j\omega_0 t + j\dot{\omega}_0 t^2/2}, \quad F(t) = \frac{\mathcal{F}(\tau_+) - \mathcal{F}(\tau_-)}{1 - j}, \quad \tau_\pm = \sqrt{2BT}\left(\pm\frac{1}{2} - \frac{t}{T}\right)$$

Show that the output of the compression filter (3.10.10) is given by

$$E_{\mathrm{compr}}(t) = \sqrt{jBT}\,\frac{\sin(\pi Bt)}{\pi Bt}\, e^{j\omega_0 t}$$

3.13 *Computer Experiment—Pulse Compression.* Take $T = 30$, $B = 4$, $f_0 = 0$. Plot the real parts of the signals $E(t)$ and $E_{\mathrm{compr}}(t)$ of the previous problem versus t over the interval $-T \le t \le T$. Some example graphs are shown in Fig. 3.12.1.

3.14 Consider the following chirped pulse, where $\dot{\omega}_0 = 2\pi B/T$:

$$E(t) = \frac{\sin(\pi t/T)}{\pi t/T}\, e^{j\omega_0 t + j\dot{\omega}_0 t^2/2}$$

Show that the output of the compression filter (3.10.10) is given by

$$E_{\mathrm{compr}}(t) = \sqrt{jBT}\, e^{j\omega_0 t - j\dot{\omega}_0 t^2/2}\,\mathrm{rect}(Bt)$$

Moreover, show that the spectrum of $E(t)$ is given in terms of the Fresnel function $\mathcal{F}(x)$ as follows:

$$\hat{E}(\omega) = \frac{\mathcal{F}(w_+) - \mathcal{F}(w_-)}{1 - j}, \quad w_\pm = \sqrt{\frac{2}{BT}}\left(\pm\frac{1}{2} - (f - f_0)T\right)$$

3.15 *Computer Experiment—Pulse Compression.* Take $T = 30$, $B = 4$, $f_0 = 0$.

a. Plot the real parts of the signals $E(t)$ and $E_{\mathrm{compr}}(t)$ of the previous problem over the interval $-T \le t \le T$. Some example graphs are shown in Fig. 3.12.2.

b. Plot the magnitude spectrum $|\hat{E}(\omega)|$ in dB versus frequency over the interval $-B/2 \le f \le B/2$ (normalize the spectrum to its maximum at $f = f_0$.) Verify that the spectrum lies essentially within the desired bandwidth B and determine its 4-dB width.

c. Write $\hat{E}(\omega)$ in the form:

$$\hat{E}(\omega) = e^{-j(\omega-\omega_0)^2/2\dot{\omega}_0} D(\omega), \quad D(\omega) = \frac{\mathcal{F}(w_+) - \mathcal{F}(w_-)}{1-j} e^{j(\omega-\omega_0)^2/2\dot{\omega}_0}$$

Plot the residual phase spectrum $\text{Arg}[D(\omega)]$ over the above frequency interval. Verify that it remains essentially flat, confirming that the phase of $\hat{E}(\omega)$ has the expected quadratic dependence on ω. Show that the small residual constant phase is numerically equal to the phase of the complex number $(1+j)\mathcal{F}(1/\sqrt{2BT})$.
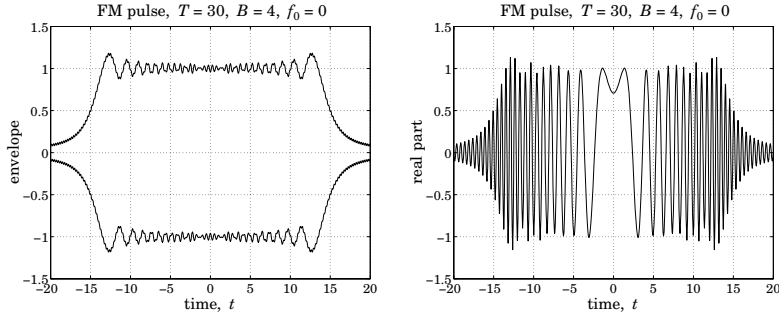

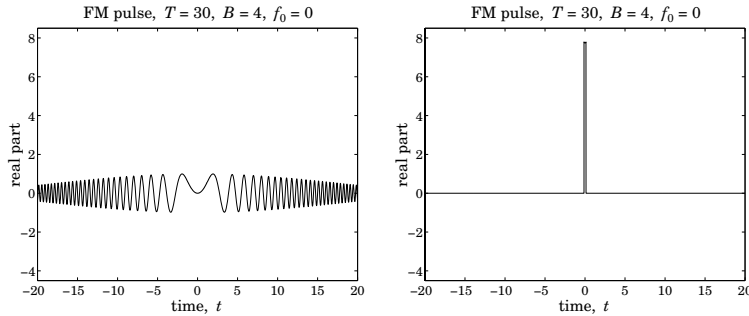
Fig. 3.12.1 Example graphs for Problem 3.13.

Fig. 3.12.2 Example graphs for Problem 3.15.

3.16 Consider the chirped gaussian pulse of effective duration T, where $\dot{\omega}_0 = \Omega/T$:

$$E(t) = e^{-t^2/2T^2} e^{j\omega_0 t + j\dot{\omega}_0 t^2/2}, \quad -\infty < t < \infty$$

Show that the output of the compression filter (3.10.10) is given by

$$E_{\text{compr}}(t) = \sqrt{j\Omega T}\, e^{j\omega_0 t - j\dot{\omega}_0 t^2/2}\, e^{-\Omega^2 t^2/2}$$

which has an effective duration of $1/\Omega$. Show that the spectrum of $E(t)$ is given by:

$$\hat{E}(\omega) = \sqrt{\frac{2\pi j}{\dot{\omega}_0}}\, e^{-j(\omega-\omega_0)^2/2/\dot{\omega}_0} \sqrt{\frac{\Omega T}{\Omega T + j}} \exp\left[-\frac{(\omega-\omega_0)^2}{2\dot{\omega}_0(\Omega T + j)}\right]$$

Show that in the limit of large time-bandwidth product, $\Omega T \gg 1$, the last exponential factor becomes

$$\exp\left[-\frac{(\omega-\omega_0)^2}{2\Omega^2}\right]$$

which shows that the effective width of the chirped spectrum is Ω.

3.17 *Stationary-Phase Approximation.* Consider a radar waveform $E(t) = F(t)e^{j\theta(t)}$, with envelope $F(t)$ and phase $\theta(t)$.

a. Using the stationary-phase approximation of Eq. (F.22) of Appendix F, show that the spectrum of $E(t)$ can be expressed approximately as:

$$\hat{E}(\omega) = \int_{-\infty}^{\infty} F(t) e^{j\theta(t)} e^{-j\omega t}\, dt \simeq \sqrt{\frac{2\pi j}{\ddot{\theta}(t_\omega)}}\, E(t_\omega) e^{-j\omega t_\omega} = \sqrt{\frac{2\pi j}{\ddot{\theta}(t_\omega)}}\, F(t_\omega) e^{j\theta(t_\omega)} e^{-j\omega t_\omega}$$

where t_ω is the solution of the equation $\dot{\theta}(t) = \omega$, obtained by applying the stationary-phase approximation to the phase function $\phi(t) = \theta(t) - \omega t$.

b. For the case of a linearly chirped signal $E(t) = F(t) e^{j\omega_0 t + j\dot{\omega}_0 t^2/2}$, show that the above approximation reads:

$$\hat{E}(\omega) \simeq \sqrt{\frac{2\pi j}{\dot{\omega}_0}}\, F\left(\frac{\omega-\omega_0}{\dot{\omega}_0}\right) e^{-j(\omega-\omega_0)^2/2\dot{\omega}_0}$$

Thus, it has the usual quadratic phase dispersion. Show that if $F(t)$ has finite duration over the time interval $|t| \leq T/2$, then, the above approximate spectrum is sharply confined within the band $|\omega - \omega_0| \leq \Omega/2$, with bandwidth $\Omega = \dot{\omega}_0 T$.

c. Consider the inverse Fourier transform of the above expression:

$$\frac{1}{2\pi} \int_{-\infty}^{\infty} \sqrt{\frac{2\pi j}{\dot{\omega}_0}}\, F\left(\frac{\omega-\omega_0}{\dot{\omega}_0}\right) e^{-j(\omega-\omega_0)^2/2\dot{\omega}_0} e^{j\omega t}\, d\omega$$

Define the phase function $\phi(\omega) = \omega t - (\omega-\omega_0)^2/2\dot{\omega}_0$. By applying the stationary-phase approximation to the above integral with respect to the phase function $\phi(\omega)$, show that the above inverse Fourier transform is precisely equal to the original chirped signal, that is, $E(t) = F(t) e^{j\omega_0 t + j\dot{\omega}_0 t^2/2}$.

d. Apply the compression filter (3.10.10) to the approximate spectrum of Part b, and show that the corresponding compressed signal is in the time domain:

$$E_{\text{compr}}(t) = \sqrt{\frac{j\dot{\omega}_0}{2\pi}}\, e^{j\omega_0 t}\, \hat{F}(-\dot{\omega}_0 t)$$

where $\hat{F}(\omega)$ is the Fourier transform of $F(t)$. This is similar, but not quite identical, to the exact expression (3.10.14).

e. Show that Part c is a general result. Consider the stationary-phase approximation spectrum of Part a. Its inverse Fourier transform is:

$$\frac{1}{2\pi} \int_{-\infty}^{\infty} \sqrt{\frac{2\pi j}{\ddot{\theta}(t_\omega)}}\, F(t_\omega) e^{j\theta(t_\omega)} e^{-j\omega t_\omega} e^{j\omega t}\, d\omega$$
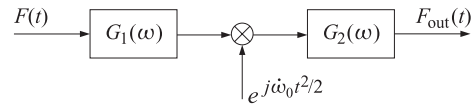
Define the phase function $\phi(\omega) = \theta(t_\omega) - \omega t_\omega + \omega t$. Show that the stationary-phase approximation applied to this integral with respect to the phase function $\phi(\omega)$ recovers the original waveform $E(t) = F(t) e^{j\theta(t)}$.

[*Hint:* the condition $\dot{\theta}(t_\omega) = \omega$ implies $\ddot{\theta}(t_\omega)(dt_\omega/d\omega) = 1$.]

3.18 An envelope signal $F(t)$ is processed through two successive pulse compression filters with
chirping parameters $\dot\omega_1$ and $\dot\omega_2$, as shown below.

where $G_i(\omega) = e^{j\omega^2/2\dot\omega_i}$, $i = 1, 2$. Show that if the chirping parameter of the intermediate
quadratic modulation is chosen to be $\dot\omega_0 = \dot\omega_1 + \dot\omega_2$, then the overall output is a time-scaled
version of the input:

$$F_{\text{out}}(t) = j\sqrt{\frac{\dot\omega_2}{\dot\omega_1}}\, e^{j\dot\omega_0\dot\omega_2 t^2/2\dot\omega_1}\, F\left(-\frac{\dot\omega_2 t}{\dot\omega_1}\right)$$